

## Journal Pre-proofs

The Discovery of Quinoline Derivatives, as NF- $\kappa$ B Inducing Kinase (NIK) Inhibitors with Anti-inflammatory Effects in Vitro, Low Toxicities against T Cell Growth

Jianing Song, Yuqin Zhu, Weidong Zu, Chunqi Duan, Junyu Xu, Fei Jang, Xinren Wang, Shuwen Li, Chenhe Liu, Qianqian Gao, Hongmei Li, Yanmin Zhang, Weifang Tan, Tao Lu, Yadong Chen

PII: S0968-0896(20)30686-6  
DOI: <https://doi.org/10.1016/j.bmc.2020.115856>  
Reference: BMC 115856

To appear in: *Bioorganic & Medicinal Chemistry*

Received Date: 11 September 2020  
Revised Date: 29 October 2020  
Accepted Date: 1 November 2020

Please cite this article as: J. Song, Y. Zhu, W. Zu, C. Duan, J. Xu, F. Jang, X. Wang, S. Li, C. Liu, Q. Gao, H. Li, Y. Zhang, W. Tan, T. Lu, Y. Chen, The Discovery of Quinoline Derivatives, as NF- $\kappa$ B Inducing Kinase (NIK) Inhibitors with Anti-inflammatory Effects in Vitro, Low Toxicities against T Cell Growth, *Bioorganic & Medicinal Chemistry* (2020), doi: <https://doi.org/10.1016/j.bmc.2020.115856>

This is a PDF file of an article that has undergone enhancements after acceptance, such as the addition of a cover page and metadata, and formatting for readability, but it is not yet the definitive version of record. This version will undergo additional copyediting, typesetting and review before it is published in its final form, but we are providing this version to give early visibility of the article. Please note that, during the production process, errors may be discovered which could affect the content, and all legal disclaimers that apply to the journal pertain.

© 2020 Published by Elsevier Ltd.



# The Discovery of Quinoline Derivatives, as NF- $\kappa$ B Inducing Kinase (NIK) Inhibitors with Anti- inflammatory Effects in Vitro, Low Toxicities against T Cell Growth

*Jianing Song<sup>§,†</sup>, Yuqin Zhu<sup>†,‡</sup>, Weidong Zu<sup>†</sup>, Chunqi, Duan<sup>†</sup>, Junyu Xu<sup>†</sup>, Fei Jang<sup>†</sup>, Xinren Wang<sup>†</sup>, Shuwen Li<sup>†</sup>, Chenhe Liu<sup>†</sup>, Qianqian Gao<sup>†</sup>, Hongmei Li<sup>†</sup>, Yanmin Zhang<sup>†</sup>, Weifang Tan<sup>†</sup>, Tao Lu<sup>\*†,§</sup>, Yadong Chen<sup>\*†</sup>.*

<sup>†</sup>School of Sciences, China Pharmaceutical University, 639 Longmian Avenue, Nanjing 211198, PR China.

<sup>§</sup>State Key Laboratory of Natural Medicines, China Pharmaceutical University, 24 Tongjiaxiang, Nanjing 210009, PR China.

## ABSTRACT

NIK is a critical regulatory protein of the non-classical NF- $\kappa$ B pathway, and its dysregulated activation has been proved to be one of the pathogenic factors in a variety of autoimmune diseases and inflammatory diseases. Nevertheless, its corresponding development of inhibitors faces many obstacles, including the lack of structure types of known inhibitors, immature activity evaluation methods of compounds in vitro. In this study, a series of quinoline derivatives were obtained through rational design and chemical synthesis. Among them, the representative compounds **17c** and **24c** have excellent inhibitory activities on LPS-induced macrophage (J774) nitric oxide release and anti-Con A-stimulated primary T cell proliferation. This evaluation method has good universality and overcomes the obstacles mentioned above, which are faced by the current inhibitor research to a certain extent. Besides, the compound's toxicity against the growth of T cells under non-stress conditions was evaluated, for the first time, as an indicator for the investigation to avoid potential safety risks. Pharmacokinetic properties evaluation of the less toxic compound **24c** confirmed its good metabolic behavior (especially oral properties, F% = 21.7 %), and subsequent development value.

## INTRODUCTION

The nuclear factor- $\kappa$ B (NF- $\kappa$ B) belongs to a family of inducible transcription factors, which consists of five structurally related members, including NF- $\kappa$ B1 (p50 / p105), NF- $\kappa$ B2 (p52 / p100), RelA (p65), RelB and c-Rel.<sup>1</sup> NF- $\kappa$ B family is a key mediator for regulating innate and adaptive immunity.<sup>3, 4</sup> NF- $\kappa$ B regulates the survival and activation of lymphocytes, which is essential for the normal maintenance of immune response.<sup>5</sup> Once NF- $\kappa$ B dysfunction, it will lead to constitutive activation of the NF- $\kappa$ B signaling pathway. As a result, it mediates the occurrence and progression of related autoimmune diseases and inflammatory diseases, such as rheumatoid arthritis (RA), inflammatory bowel disease (IBD), multiple sclerosis (MS), psoriasis (PSO), and bronchial asthma.<sup>6, 7</sup>

The currently developed inhibitors to block NF- $\kappa$ B signaling indicate that the treatment of autoimmune and inflammatory diseases is beneficial, but it is challenging to balance therapeutic efficacy and safety.<sup>8</sup> Relevant studies showed that comprehensive and in-depth inhibition of NF- $\kappa$ B signaling might lead to serious side effects, such as liver toxicity during embryonic development, fetal malformations<sup>9</sup>, and *Listeria monocytogenes* infection (patients often have mononuclear complications of cell proliferation) caused by decreased immunity.<sup>10</sup> There is no doubt that a better elucidation of the NF- $\kappa$ B subunit involved in a specific pathological process will help develop a new generation of anti-autoimmune and inflammatory drugs with high effects, fewer side effects, and low cost. With in-depth research on the mechanism of NF- $\kappa$ B activation, several upstream kinases (such as NIK, IKK1, IKK2, and MEKK3) and downstream effector I $\kappa$ B ubiquitin E3 ligase have been identified, which can selectively regulate NF- $\kappa$ B function. Indeed, they have become promising targets for drug development.<sup>11</sup>

NIK (also known as MAP3K14), as a key regulator, participates in the response of NF- $\kappa$ B2 signaling pathway to TNF superfamily receptors such as CD40, CD27, lymphotoxin  $\beta$  receptor (LT $\beta$ R), B cell-activating factor receptor (BAFF- R), tumor necrosis factor receptor superfamily member 12A (TWEAK), etc. Under normal physiological conditions, TRAF3 connects NIK and TRAF2-clAPs E3 to form a complex, conducive to the ubiquitination of NIK protein and its degradation by the proteasome. Unlike the generally low NIK level, when

the cytokine CD40L or BAFF binds to its membrane receptor, NIK will accumulate in the cytoplasm, leading to IKK $\alpha$  phosphorylation, p100 processing, and increased p52 levels. p52 combines with RelB to form a p52 / RelB heterodimer, which then translates to the nucleus to trigger the expression of target inflammatory factors and chemokines.<sup>12</sup> The non-classical NF- $\kappa$ B pathway regulates a variety of physiological processes, including the differentiation, maturation, and survival of B cells, and immune behavior of T cells.<sup>13-15</sup> Once the NIK is dysregulated, it can promote the abnormal activation of non-canonical NF- $\kappa$ B, thereby mediating autoimmune and inflammatory diseases' occurrence and progression. Similar to the classic NF- $\kappa$ B signal, an abnormal NF- $\kappa$ B2 signal is also an important pathogenic mechanism of RA<sup>16</sup>, which is related to the high expression of NIK in patients' synovial endothelial cells.<sup>17</sup> Progressive joint injury in patients with RA involves the abnormal generation and activation of osteoclasts, and this process depends on the NF- $\kappa$ B2 signaling pathway.<sup>18</sup> Besides, the pathogenesis of RA is often accompanied by the prolongation and maturation of B cell survival, which stems from the abnormal activation of the NF- $\kappa$ B2 pathway by BAFF.<sup>19</sup> Excessive BAFF levels in SLE patients up-regulate the NF- $\kappa$ B2 signaling pathway, thereby promoting the release of auto-antibodies from B cells and affecting the pathological survival and differentiation of B cells.<sup>20</sup> NIK overexpression mediates the pathogenesis of MS, by over activating autoreactive Th1 and Th17 cells.<sup>21-22</sup> Abnormal activations of NIK can enhance mouse intestine sensitivity to rodent citrobacter and then induce enteritis.<sup>23</sup> Similarly, NIK dysfunction also has a direct or indirect induction effect in the pathogenesis of psoriasis.<sup>24-29</sup> Thus, the research of highly potent and druggable small molecule inhibitors targeting NIK protein has excellent value and prospects.<sup>29</sup>

Currently, research on NIK inhibitors is scarce, and their structure types are far from abundant (**Figure 1**). Aminopyrimidine compound **1**, as the first NIK inhibitor, was developed by Amgen.<sup>30</sup> Compound **1** has excellent inhibitory activity against NIK and can notably alleviate the symptoms of toxicity-induced hepatitis and liver injury in mouse models.<sup>31</sup> In 2017, Genentech developed carbamoyl imidazole derivatives represented by compounds **2** and **3** through high-throughput screening and structural optimization. In particular, **2** performed better in p52/RelB dimer nuclear transfer inhibition and NF- $\kappa$ B luciferase gene report assay. Besides, they also developed other series of NIK inhibitors: nicotinamide and pyrazole derivatives represented by **4** (SIM1) and **5**,

respectively. Using compound **1** (B022) as a starting point for the inhibitor design, Zhao's group developed a series of pyrrolopyrimidin-2-amine compounds.<sup>32</sup> They also provided an example of compound **6** (XT2), as a NIK inhibitor, which can effectively inhibit toxin-induced hepatitis. Our previous work demonstrated the potential of compound **7** that alleviates the disease phenotype of imiquimod-induced psoriasis model mice.<sup>29</sup> Compound **8** is unique than other inhibitors because its molecular structure does not contain alkynyl linkers and tertiary alcohol fragments used to match the back pocket's shape.

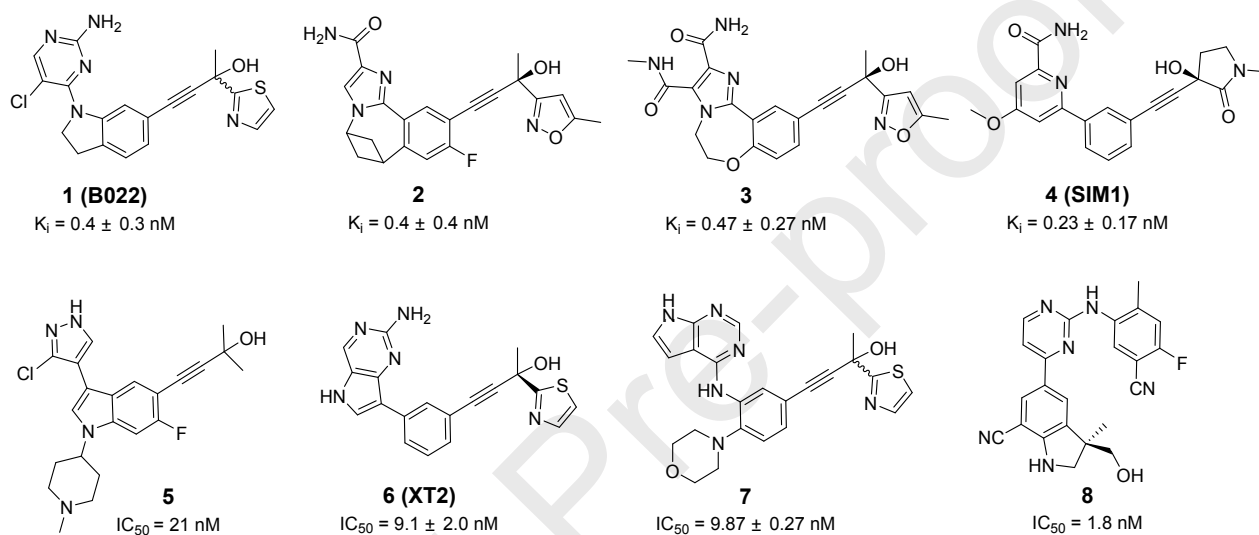


**Figure 1.** Representative NIK inhibitors.

Ignoring that the structural types of known inhibitors are scarce, their development also faces many other obstacles, including immature cell screening methods, high clearance rates of compounds, and short half-lives in vivo (compound **1**). This situation dramatically limits the verification of NIK protein's biological function and the exploration of its potential indications. Thus, the development of NIK inhibitors with high druggability and the enrichment of structural types have become the primary task.<sup>33, 34</sup> Inspired by the structure of 3-pyrazole-indole analog **5**, we speculated on the factors that may be unfavorable to its activity and developed a new design strategy in this work. Through synthetic chemical means, a series of quinoline derivatives with suitable NIK enzyme inhibitory activities were obtained. The corresponding activity evaluation revolved around their inhibitory potency against NIK, cell activity, and toxicity, and PK characteristics of the selected compounds.

## RESULTS AND DISCUSSION

## Structure-Based Design Strategy

In 2015, Janssen Pharmaceuticals developed the indole skeleton analog **5**, which has a double-digit nanomolar NIK inhibitory activity ( $IC_{50} = 21$  nM) and a good anti-proliferation activity ( $IC_{50} = 61$  nM) against human leukemia cell line (JLN3, a genetically engineered cell line transfected with NIK plasmid). Given this series compounds' excellent in vitro activities, Janssen applied for a corresponding Chinese patent. However, there is no follow-up report of further research. In order to obtain a class of novel quinoline NIK small molecule inhibitors, a new and reasonable design strategy was proposed based on **5**. As described in **Figure 2A**, the design strategy includes: a) removing negative spatial trends and the excessively sizeable 4-methyl piperidine ring. b) the pyrrole ring is grown into pyridine, gives a highly medicinal core: quinoline skeleton. This ring expansion treatment may benefit the 6-position alkynyl group to point to the back pocket region. c) Introducing a predominant group that fits well with the back pocket: the thiazolyl fragment. As can be seen from **Figure 2B**, there are two important amino residues in the back pocket, which are Asp536 and Phe537. Thiazole can adapt to its volume and may have potential interactions in hydrogen bond and  $\pi$ - $\pi$  stacking. The application of above strategy has spawned a representative quinoline derivative **17a**.

Subsequently, compound **17a** was docked into the NIK crystal structure (RCSB PDB code 4G3E) to explore the compatibility of **17a** with the NIK binding pocket (**Figure 2B**). The pyrazole fragment occupies the hinge region and forms corresponding hydrogen bond interactions with Leu474 and Glu472, respectively. With proper spatial orientation, the alkynyl group smoothly extends into the back pocket area through the narrow channel formed by the side chains of Met471, Lys431, and Asp536. The thiazole ring locates in a small hydrophobic pocket behind Met471, where the thiazole ring forms a  $\pi$ - $\pi$  stacking effect with the benzene ring of Phe537. The nitrogen atom on the thiazole ring forms a hydrogen bond interaction with Asp536. In the back pocket, the alkynol hydroxyl group captures Phe537 and Glu442 residues, forming essential hydrogen bonds. Besides, the lactam structural unit of compound **17a** (2-hydroxyquinoline tautomerism) occupies the solvent-accessible area. The cavity is not fully occupied in this area, making the 2-position of quinoline has great structural modification potential. The cross-sectional view shows the arrangement and molecular orientation

of **17a** within the binding site (**Figure 2C**). The next kinase activity assay confirmed that **17a** has a good inhibitory potency against NIK ( $IC_{50} = 38.6 \pm 0.25$  nM).

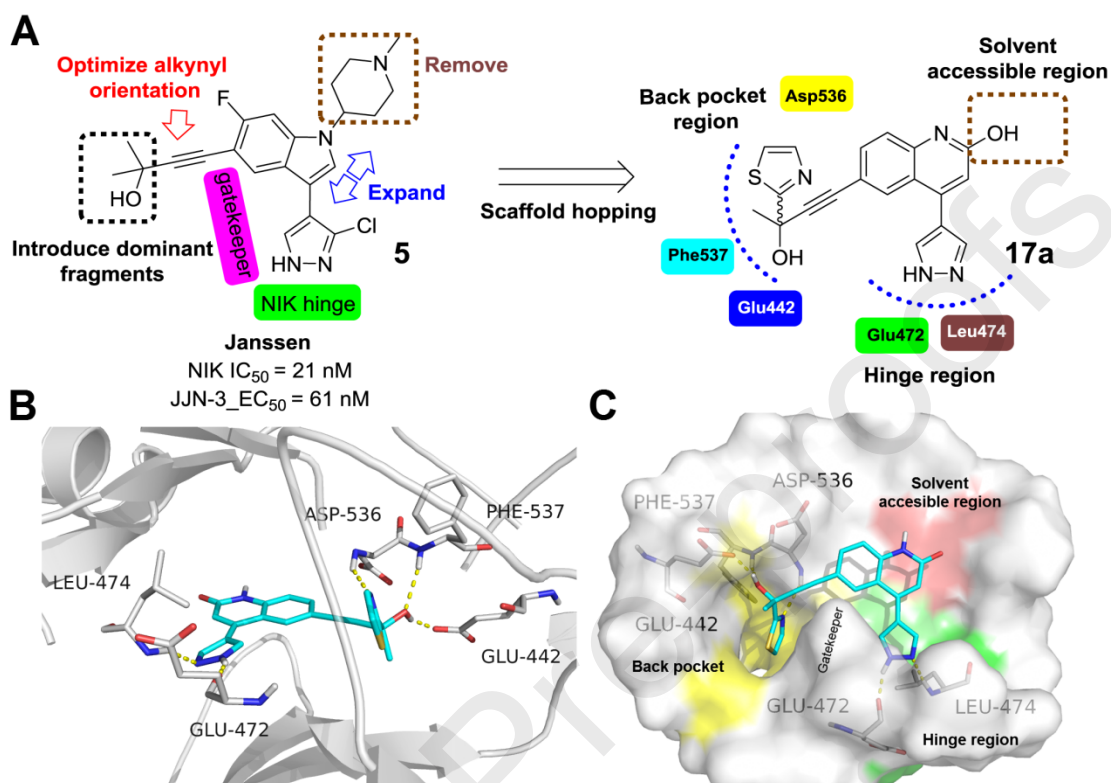


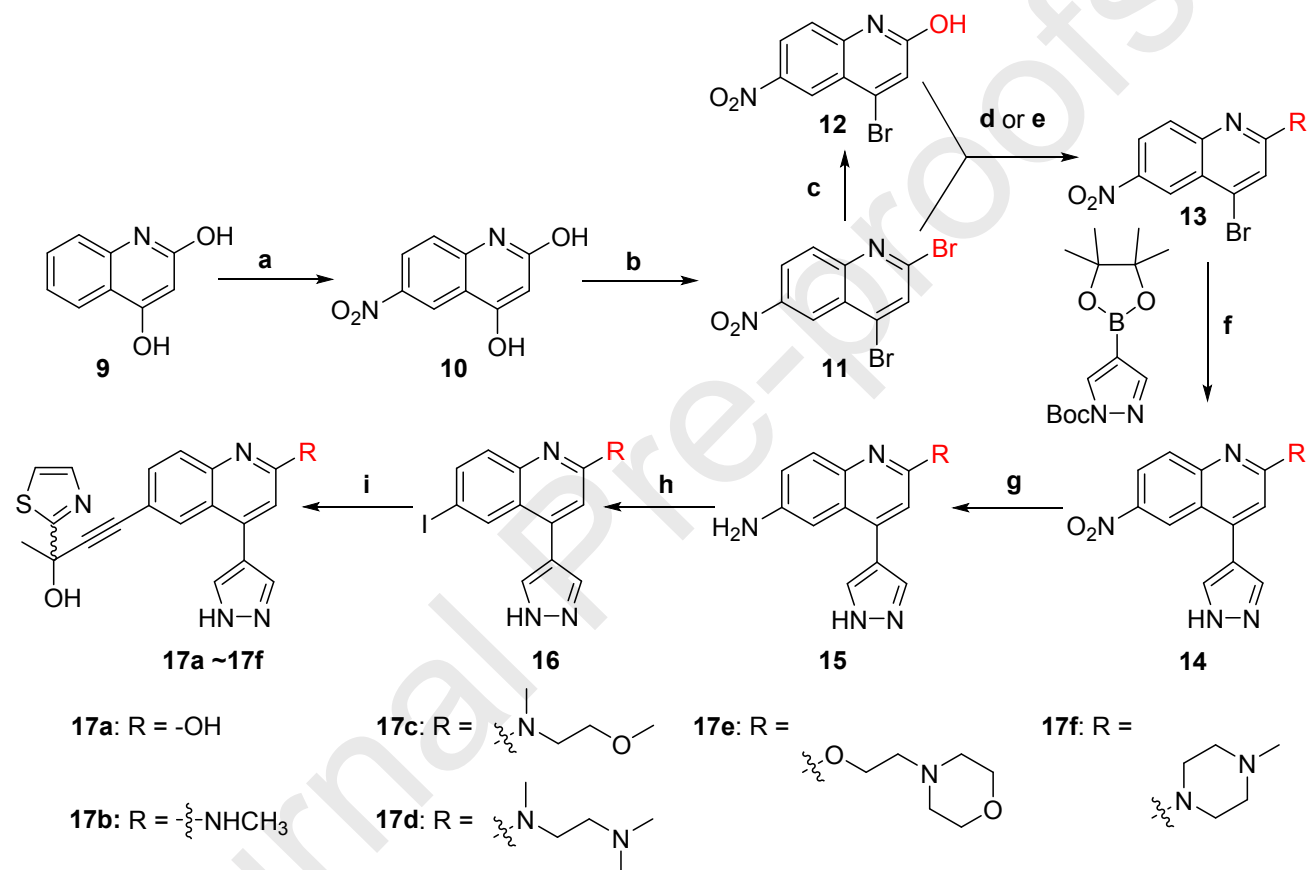
**Figure 2.** (A) Based on the structure of compound **5**, the follow-up optimization ideas are proposed. (B) Representative compound **17a** docked into NIK (PDB code 4G3E). (C) Spatial layout of **17a** in NIK binding pocket is presented (PDB code 4G3E).

## Chemistry

As presented in **Scheme 1**, using 2,4-hydroxyquinoline as the starting material, intermediate **10** was obtained in a good yield through a nitration reaction in a nitric acid/sulfuric acid reaction system. Subsequently, the 2-hydroxy group of the quinoline was substituted with bromine to give **11**. The bromine atom can be derived from phosphorus oxybromide or tetrabutylammonium bromide (step **b**). In step **c**, acetic acid catalyzed the hydrolysis of **11** to give 4-bromo-6-nitroquinolin-2-ol (**12**). Under strict reaction temperature and the dripping acceleration control of the hydrophilic group, various kinds of chain or cyclic secondary amines selectively attack the quinoline 2-position to give **13b—13d** or **13f** with high yields. For the synthesis of 4-(2-

((6-nitroquinolin-2-yl)oxy)ethyl)morpholine (**13e**), Et<sub>3</sub>N in condition **d** was replaced by NaH. Under the catalysis of PdCl<sub>2</sub>(dppf), **13** was coupled with pyrazole borate, and then, the Boc protecting group was removed by using trifluoroacetic acid to generate **14**. Subsequently, **14** undergoes three-step reaction: Fe/NH<sub>4</sub>Cl catalyzed nitro reduction reaction, Sandmeyer reaction, and Sonogashira coupling gave the final product **17a** – **17f**.

**Scheme 1.** Synthesis of 2-hydrophilic substituted quinoline analogs<sup>a</sup>

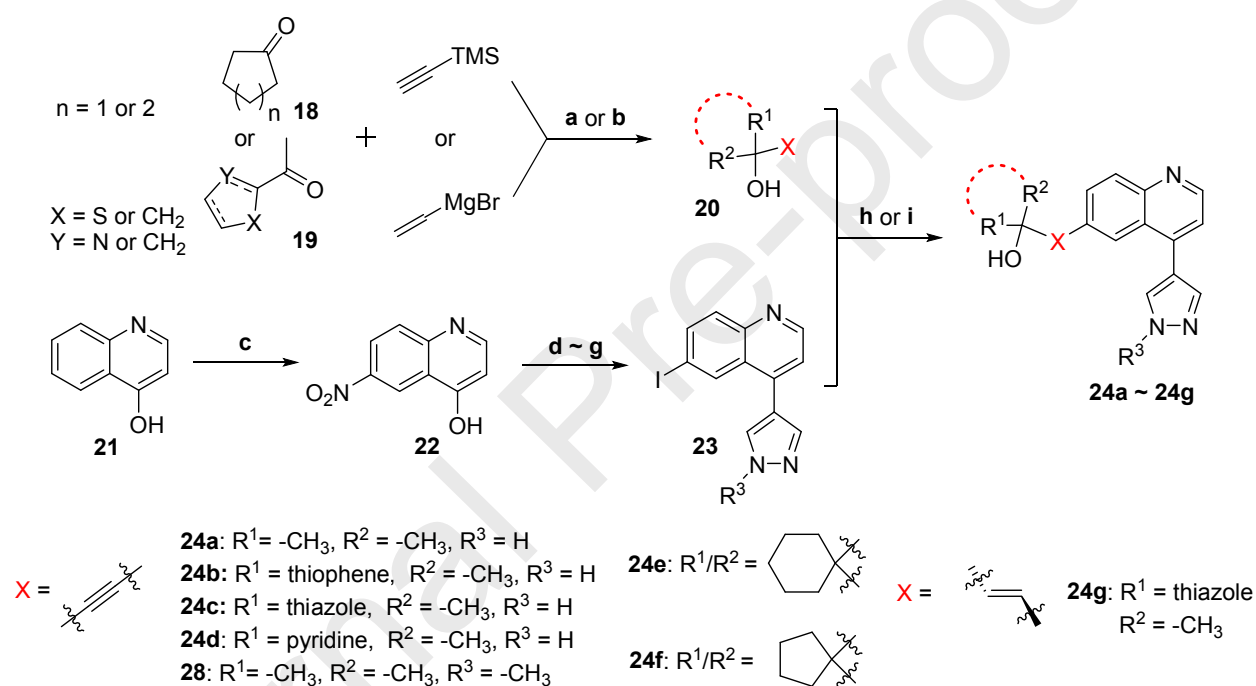


<sup>a</sup>**Reagents and conditions:** (a) HNO<sub>3</sub>, H<sub>2</sub>SO<sub>4</sub>, 0 °C; (b) POBr<sub>3</sub>, toluene, 110 °C or (n-Bu)<sub>4</sub>N<sup>+</sup>Br<sup>-</sup>, P<sub>2</sub>O<sub>5</sub>, toluene; (c) HOAc, 90 °C, overnight; (d) appropriate amine, Et<sub>3</sub>N, DCM, 0 °C; (e) NaH, corresponding 4-(2-chloroethyl)morpholine, DCM, 0 °C – room temperature; (f) PdCl<sub>2</sub>(dppf), K<sub>2</sub>CO<sub>3</sub>, dioxane/H<sub>2</sub>O, 80 °C; coupling completed, CF<sub>3</sub>COOH, DCM, r.t.; (g) Fe, NH<sub>4</sub>Cl, 75% EtOH; (h) NaNO<sub>2</sub>, KI, *p*-TsOH, CH<sub>3</sub>CN/H<sub>2</sub>O, 0 °C – room temperature; (i) 2-(thiazol-2-yl)but-3-yn-2-ol, PdCl<sub>2</sub>(PPh<sub>3</sub>)<sub>2</sub>, CuI, Et<sub>3</sub>N/THF = 1:3.

As shown in **Scheme 2**, the synthesis of different back pocket binding structural units (**20**) was achieved through the nucleophilic attack of ketones by terminal alkyne or alkenyl Grignard reagent. Similar to the

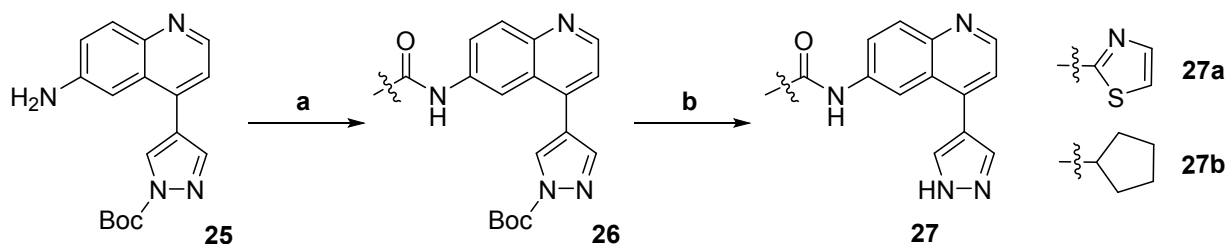
synthesis of compound **16**, 2-hydroxyquinoline was used as the starting material to synthesize intermediate **23**. Subsequently, **23** reacted with **20** in the presence of  $\text{PdCl}_2(\text{PPh}_3)_2$  and  $\text{CuI}$  to give target compounds **24a**–**24f**. Using methyl pyrazole borate, the synthesis of compound **28** was similar as that of compound **24a**. When introducing alkenyl groups as linkers (**24g**),  $\text{Pd}(\text{OAc})_2$  was required as a catalyst. In **Scheme 3**, the preparation of **27a**–**27b** was achieved by two reactions: introduction of amide linker in the presence of  $\text{Et}_3\text{N}$  as a base, and removal of the pyrazole nitrogen “-Boc” protecting group.

**Scheme 2.** Synthesis of compounds **24a–24g**<sup>a</sup>



**Reagents and conditions:** (a)  $n\text{-BuLi}$ , THF,  $-78^\circ\text{C}$  – r. t., and then  $\text{NaOH}$  (3.0 equiv) in MeOH was dropwise; (b) THF, stirred at  $0^\circ\text{C}$ ; (c)  $\text{HNO}_3$ ,  $\text{H}_2\text{SO}_4$ ,  $0^\circ\text{C}$ ; (d)  $\text{POBr}_3$ , toluene,  $110^\circ\text{C}$  or  $(n\text{-Bu})_4\text{N}^+\text{Br}^-$ ,  $\text{P}_2\text{O}_5$ , toluene; (e)  $\text{PdCl}_2(\text{dppf})$ ,  $\text{K}_2\text{CO}_3$ , dioxane/ $\text{H}_2\text{O}$ ,  $80^\circ\text{C}$ , and then  $\text{CF}_3\text{COOH}$ , DCM, r. t.; (f)  $\text{Fe}$ ,  $\text{NH}_4\text{Cl}$ , 75% EtOH; (g)  $\text{NaNO}_2$ , KI,  $p\text{-TsOH}$ ,  $\text{CH}_3\text{CN}/\text{H}_2\text{O}$ ,  $0^\circ\text{C}$  – room temperature; (h)  $\text{PdCl}_2(\text{PPh}_3)_2$ ,  $\text{CuI}$ ,  $\text{Et}_3\text{N}/\text{THF} = 1:3$ ; (i)  $\text{Pd}(\text{OAc})_2$ ,  $\text{PPh}_3$ ,  $\text{K}_2\text{CO}_3$ , toluene,  $90^\circ\text{C}$ , overnight.

**Scheme 3.** Synthesis of compounds **27a–27c**<sup>a</sup>

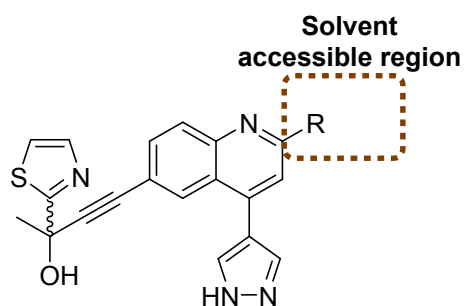


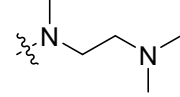
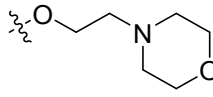
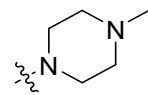
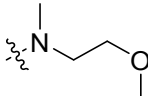
**Reagents and conditions:** (a) appropriate acyl chloride, Et<sub>3</sub>N, DMF, 0 °C; (b) CF<sub>3</sub>COOH, DCM, room temperature.

### Structure-Activity-Relationship (SAR) Studies

Taking **17a** as the starting point of structural modification, the introduction of a larger volume of methylamino at the 2-position of quinoline gave **17b**, and its activity was slightly improved compared to the former. Replacement of the methylamino group with different flexible hydrophilic substituents greatly affects the NIK inhibitory activities of compounds (**17c** and **17d**). Among them, the inhibition of **17c** towards NIK was significantly improved (IC<sub>50</sub> = 5.2 ± 0.04 nM). However, when the terminal of a flexible hydrophilic group was substituted with dimethylamino (**17d**), its activity decreased, which might be due to repulsion between the terminal methyl group and amino acid residues surrounding protein cavity at this position (**Figure 3**). Subsequently, cyclization of the terminal dimethylamino group of **17d** to a morpholine ring obtained **17e**. It was found that its inhibitory effect against NIK was almost lost, indicating the reasonableness and reliability of the above speculation. To further investigate the volume of the cavity in the solvent accessible area, the methyl piperazine ring was introduced into the quinoline 2-position to generate the compound **17e**, which retained the potency on NIK (compare **17d** with **17f**).

**Table 1.** Structure optimization of 2-position substituents of quinoline in solvent accessible region



Compounds	R	NIK IC <sub>50</sub> (nM) <sup>a</sup>	Compounds	R	NIK IC <sub>50</sub> (nM) <sup>a</sup>
					% enzyme activity <sup>b</sup>
<b>1</b>	/	4.9 ± 0.34	<b>17d</b>		159.6 ± 1.13
<b>17a</b>	-OH	38.6 ± 0.25	<b>17e</b>		91.97±0.24%
<b>17b</b>	-NHCH <sub>3</sub>	26.0 ± 0.18	<b>17f</b>		174.8 ± 0.97
<b>17c</b>		5.2 ± 0.04			

<sup>a</sup>Kinase inhibition assay was performed at 10 μM ATP concentration, and the values are the mean ± SD from two independent experiments. <sup>b</sup>Enzyme activity assay was investigated at 2 μM dosing compound concentration and 10 μM ATP concentration.

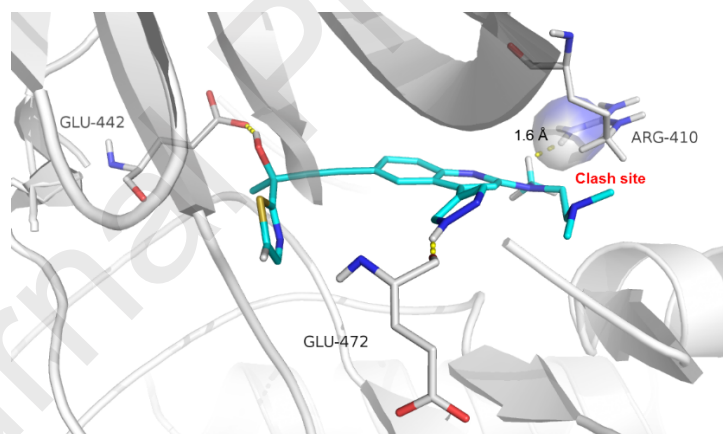
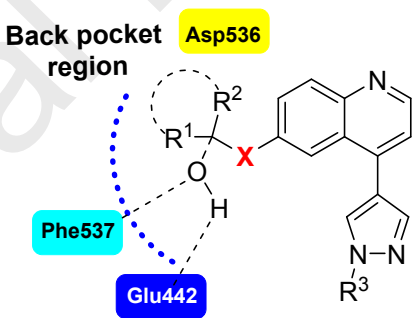


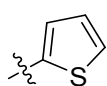
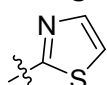
**Figure 3.** Representative compound **17d** docked into NIK (PDB code 4G3E).

Further work mainly investigated the match of different tertiary alcohol fragments to the back pocket and the types and characteristics of linker structures that can smoothly pass through the narrow channels formed by the side chains of Met471, Lys431, and Asp536. As shown in **Table 2**, a variety of tertiary alcohol fragments with different shapes, sizes, and electrical properties were preferentially investigated. When R<sup>1</sup> and R<sup>2</sup> were methyl groups (**24a**), the activity was greatly reduced. Substitution of methyl group with five-membered, or

six-membered aromatic ring afforded **24b** – **24d**. Summarizing the corresponding activity data showed that five- or six-membered aromatic rings are conducive to the improvement of activities. Specifically, compound **24c** more potently inhibits the protein activity of NIK ( $IC_{50} = 22.1 \pm 2.46$  nM), demonstrating the importance of the hydrogen bonding interaction between the thiazole nitrogen atom and Asp536 (compare **24b** with **24c**). The cyclization of  $R^1$  and  $R^2$ , as a six-membered saturated aliphatic ring, reduces the activity of **24e** (compare to **24f**) by nearly 10-fold, which may be due to its excessive bulk. Subsequently, the alkynyl group was replaced with a different linker to investigate the linker characteristics that can smoothly pass through narrow channel of the back pocket. Using vinyl as a linker (**24g**,  $IC_{50} = 2080$  nM), the activity was decreased by nearly 100-fold (compare **24g** with **24c**). The more flexible amide bond as a linker is unfavorable for binding between the corresponding compound and the NIK active pocket (compare **27a** or **27b** with **24f**). Besides, methylation blocks "-NH-" on the pyrazole structural unit, resulting in the complete loss of the activity of compound **28**, which verifies the importance of hydrogen bonding interaction in hinge region to maintain good ligand NIK inhibitory activity.

**Table 2.** Structures and their inhibitory activities against NIK of target compounds



Compounds	$R^1$	$R^2$	X	$R^3$	NIK $IC_{50}$ (nM) <sup>a</sup>
					% enzyme activity <sup>b</sup>
<b>24a</b>	-CH <sub>3</sub>	-CH <sub>3</sub>		H	1720 ± 32.16
<b>24b</b>		-CH <sub>3</sub>		H	523.8 ± 12.57
<b>24c</b>		-CH <sub>3</sub>		H	22.1 ± 2.46

24d		-CH <sub>3</sub>		H	590.9 ± 21.47
24e				H	6050 ± 76.25
24f				H	564.1 ± 16.3
24g		-CH <sub>3</sub>		H	2080 ± 24.83
27a				H	72.26 ± 1.26%
27b				H	83.60 ± 1.37%
28	-CH <sub>3</sub>	-CH <sub>3</sub>		-CH <sub>3</sub>	99.09 ± 0.08%

<sup>a</sup>Kinase inhibition assay was performed at 10  $\mu$ M ATP concentration, and the values are the mean  $\pm$  SD from two independent experiments. <sup>b</sup>Enzyme activity assay was investigated at 2  $\mu$ M dosing compound concentration and 10  $\mu$ M ATP concentration.

### Inhibitory Activities of the Compounds on the Release of Nitric Oxide (NO) in J774 Macrophages and Anti-splenic T cell Proliferation Activities

In the pathogenesis of various autoimmune and inflammatory diseases (such as RA, SLE, and PSO), NIK's dysregulated activation can regulate the prolonged survival of B cells, excessive proliferation of T cells, and deepened infiltration of macrophages.<sup>20-22, 29</sup> Thus, investigation of the compounds' inhibitory effects on lipopolysaccharide (LPS) induced NO release in macrophages, and concanavalin A (Con A) stimulated splenic T cell proliferation is of great significance for evaluating its cell activity. Six compounds with better NIK inhibitory potency (**17a** – **17d**, **17f**, and **24c**) were selected for further cell-level activity assay. The results showed that at 1  $\mu$ M concentration, four compounds inhibited LPS-induced NO release in J774 cells by more than 40%. Consistent with its high enzyme inhibitory efficacy, the activity of **17c** was optimal at 51%, which indicated that the introduction of appropriate flexible hydrophilic groups might increase the inhibition of NO release of in J774 cells. In other parallel experiments, these compounds all showed notably anti-T cell proliferation activities

at two dose levels (2  $\mu$ M and 0.4  $\mu$ M). Interestingly, although there is an apparent distinction between **17c** and **24c** in inhibitory activities on NIK enzyme and macrophage NO release, their T cell anti-proliferative activities of both performed better, and the inhibitory efficacy were similar.

**Table 3.** Anti-inflammatory activity screening of selected compounds at cellular level.

Cpds	NIK IC <sub>50</sub> (nM)	NO Inhibition rate (%) <sup>a</sup>		
		At 1 $\mu$ M	At 2 $\mu$ M	At 0.4 $\mu$ M
<b>1</b>	4.9 $\pm$ 0.34	43.90 $\pm$ 0.12	59.57 $\pm$ 0.09	19.04 $\pm$ 0.03
<b>17a</b>	38.6 $\pm$ 0.25	31.45 $\pm$ 0.34	27.25 $\pm$ 0.44	23.31 $\pm$ 0.03
<b>17b</b>	26.0 $\pm$ 0.18	46.48 $\pm$ 0.75	34.50 $\pm$ 0.88	18.40 $\pm$ 0.68
<b>17c</b>	5.2 $\pm$ 0.04	51.44 $\pm$ 0.58	53.13 $\pm$ 0.22	33.05 $\pm$ 0.49
<b>17d</b>	159.6 $\pm$ 1.13	34.63 $\pm$ 0.28	22.72 $\pm$ 0.34	19.93 $\pm$ 0.81
<b>17f</b>	174.8 $\pm$ 0.97	41.03 $\pm$ 0.70	36.72 $\pm$ 0.08	19.38 $\pm$ 0.12
<b>24c</b>	22.1 $\pm$ 2.46	43.77 $\pm$ 0.74	52.46 $\pm$ 0.71	36.14 $\pm$ 0.84

<sup>a</sup>NO inhibition rate % = (model group NO concentration – compound group NO concentration) / (model group NO concentration – control group NO concentration)  $\times$  100%. <sup>b</sup>The proliferation of splenic T cells induced by Con A was tested under the treatment of six selected compounds. Proliferation -Inhibitory rate (%) = (test hole absorbance – blank hole absorbance) / (control hole absorbance – blank hole absorbance)  $\times$  100%. <sup>a,b</sup>The values are the mean  $\pm$  SD from three independent experiments, n = 3.

### Toxicity of Representative Compounds for Normal Growth and Differentiation of Splenic T Cells

As an important indicator for the evaluation of anti-inflammatory small molecule inhibitors, the lower toxicity of the compound to normal growth and differentiation of T cells (non-Con A stimulation), the higher its subsequent development potential. It is expected that small molecules can target to suppress the expression of inflammation-related target genes and the secretion of inflammatory cytokines in immune cells, instead of directly killing immune cells to eliminate inflammation.<sup>35</sup> Taking compound **1** developed by Amgen and compound **7** discovered in another part of our work as positive drugs, we examined the T cell growth toxicity of six compounds in this series. As shown in **Figure 4**, the compounds' T cell toxicity is different from each other. Among them, the toxicity of **17c** and **17f** is similar to that of compound **1**, and the inhibition rate is close to 30%. Besides, the **17d** and **24c** toxicity performance were comparable to **1**, and both were low. **17a** did not

show toxicity, and the T cells grew well in this administration group. Besides, the compound **17c**, which has the best cell activity, is about three times as toxic as the positive compound **7**. Integrating the above macrophage, T cell activity, and growth toxicity data of compounds found that **24c** is a highly active and less toxic compound. Accordingly, **24c** can be selected for the subsequent determination of metabolic stability and pharmacokinetic parameters in SD rats.

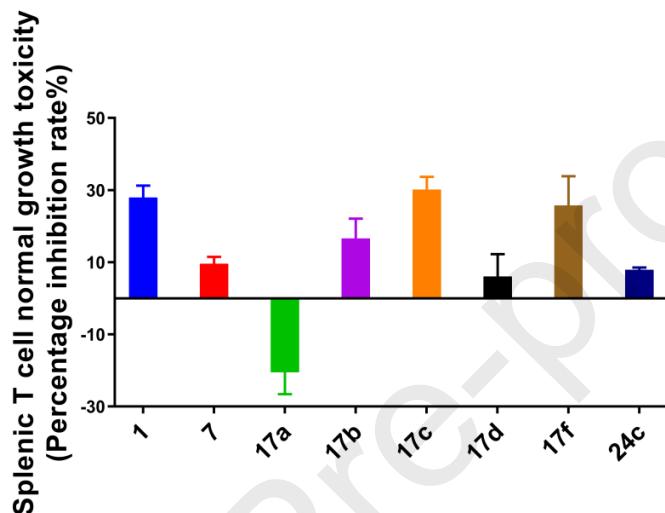


**Figure 4.** Using known NIK inhibitors **1** and **7** as the positive control group, the toxicity of selected six compounds on T cells' normal growth at a concentration of 10  $\mu$ M was investigated. Proliferation - inhibitory rate (%) = (test hole absorbance – blank hole absorbance) / (control hole absorbance – blank hole absorbance)  $\times$  100%. The values are the mean  $\pm$  SD from three independent experiments, n = 3.

### Multi-Species Liver Microsomal Metabolic Stability and In Vivo Pharmacokinetic (PK) Parameters of Compound **24c**

As shown in **Table 4**, we evaluated the metabolic stability of **24c** in human liver microsomes (HLM), monkey liver microsomes (MLM), dog liver microsomes (DLM), and rat liver microsomes (RLM). **24c** has moderate metabolic stability of human liver microsomes, and its clearance rate was 40.237 mL/min/kg. When switching to monkey-derived liver microsomes, the compound's metabolic half-life was basically maintained ( $T_{1/2}$  = 33.185 min), but the clearance rate increased to 60.156 mL/min/kg. Inconsistently, in dog and rat liver microsomes, the stability of **24c** decreased significantly, which corresponds to the clearance data in the liver

microsomes of these two species. The data presented in **Table 5** show the pharmacokinetic performance of **24c** under two administration modes: intravenous (IV) and oral (PO). When test compound **24c** (1.0 mg/kg) was injected into the tail vein, the  $C_0$  was as high as 1003 ng/mL, the area under the curve was good ( $AUC_{0-\infty} = 408$  ng h/mL), and the half-life was slightly shorter ( $T_{1/2} = 0.382$  h) accompanied by a moderate clearance rate. Correspondingly, at 0.9 h after oral gavage (i.g.) administration of compound **24c**, plasma concentration reached the maximum. Besides, the area under the curve ( $AUC_{0-\infty} = 885$  ng h/mL) did not reach the ideal, and the half-life was 1.19 h. It is worth mentioning that the oral bioavailability of **24c** ( $F\% = 21.7\%$ ) is acceptable, promoting its potential for follow-up research. Based on its good activities in vitro, low T cell survival toxicity, and acceptable PK properties, compound **24c** may be considered to explore the potentially applicable symptoms of NIK dysregulation or overexpression and verify its related biological mechanisms.

**Table 4.** Metabolic stability of compound **24c** in liver microsomes of multiple species

Compound	Species	$R^2$ <sup>a</sup>	$T_{1/2}$ (min) <sup>b</sup>	$CL_{int, \text{microsome}}$ ( $\mu\text{L}/\text{min}/\text{mg}$ proteins) <sup>c</sup>	$CL_{int, \text{in vivo}}$ (mL/min/kg) <sup>d</sup>
<b>24c</b>	Human	0.9999	33.099	42.579	40.237
	Monkey	0.9922	33.185	41.775	60.156
	Dog	0.9983	14.224	97.451	140.330
	Rat	0.9917	12.554	110.427	198.768

<sup>a</sup> $R^2$  is the correlation coefficient of the linear regression for determination of the kinetic constant. <sup>b</sup>Elimination half-life ( $T_{1/2}$ ). <sup>c</sup>Intrinsic clearance in LMs ( $CL_{int, \text{in vitro}}$ ), <sup>d</sup>Intrinsic hepatic clearance ( $CL_{int, \text{in vivo}}$ ).  $CL_{int, \text{in vivo}} = CL_{int, \text{in vitro}}$  (mL/min/mg microsomal protein)  $\times$  Scaling factor (physiological parameter) =  $CL_{int, \text{in vitro}}$  (mL/min/mg microsomal protein)  $\times$  Microsomal protein (mg protein/g liver)  $\times$  Liver weight (g liver/kg body weight).

**Table 5.** Pharmacokinetic parameters of compound **24c** in Sprague Dawley Rat<sup>a</sup>

PK parameters (n=3) <sup>b</sup>	IV (1.0 mg/Kg)		PK parameters (n=3) <sup>a</sup>	PO (10 mg/Kg)	
		SD			SD
$AUC(0-\infty)(\text{ng}\cdot\text{h}/\text{mL})$	408	126	$AUC(0-\infty)(\text{ng}\cdot\text{h}/\text{mL})$	885	137

<b>C<sub>0</sub> (ng/mL)</b>	1003	113	<b>C<sub>max</sub> (ng/mL)</b>	311	92
<b>T<sub>1/2</sub> (h)</b>	0.382	0.087	<b>T<sub>1/2</sub> (h)</b>	1.19	0.194
<b>V<sub>d</sub> (L/kg)</b>	2.73	0.393	<b>T<sub>max</sub> (h)</b>	0.900	0.173
<b>CL (mL/kg/min)</b>	43.3	12.2	<b>F(%)</b>	21.7	3.3

<sup>a</sup>After intravenous injection (i.v., 1.0 mg / kg) or gavage (i.g., 10 mg / kg) of compound **24c**, the blood concentration of mice was recorded over time. Corresponding in vivo pharmacokinetic parameters are given. Injection formulation (prescription, DMSO : PEG200 : Saline = 20 : 20 : 60, v / v / v. concentration, 0.2 mg·mL<sup>-1</sup>). Oral formulation (0.5% CMC-Na / 0.2% Tween 80. concentration, 1 mg·mL<sup>-1</sup>). <sup>b</sup>PK parameters are the mean ± SD from three independent experimental rats, n = 3.

## CONCLUSIONS

Inspired by the structure of 3-pyrazole-indole analog **5**, a further design strategy was put forward. The structural activity modification revolves around the following aspects: a) The introduction of flexible chain-like and cyclic hydrophilic moieties with different sizes at the 2-position of quinoline to explore the characteristics of the solvent-accessible region. b) Investigation and verification of the dominant fragments of the back pocket. c) Replacement of alkynyl linker. Subsequently, compounds **17c** and **24c** attracted our attention for their outstanding inhibitory potency against NIK and cell activities. Further, T cell toxicity analysis confirmed that **17c** performed poorly, and the toxicity was significantly higher than that of control groups (compounds **1** and **7**). The cross-species liver microsomal metabolism stability of **24c** in vitro and SD rat pharmacokinetics (PK) properties in vivo are acceptable, especially its oral properties (F% = 21.7%), which prompts it has the potential for subsequent development. In short, a series of quinoline derivatives, with potent NIK inhibition, developed in this work have enriched the structural types of inhibitors to a certain extent. Two inflammatory cell models were constructed: LPS-induced (J774) NO release in macrophages and Con A-stimulated splenic T cell proliferation. This screening technique has certain universality. Besides, the toxicity study of NIK inhibitors is included in the evaluation system, which may help to avoid the toxicity problems of inhibitors and reduce the risk of development.

## EXPERIMENTAL SECTION

### **ADP-Glo™ Kinase Inhibition Assay**

The kinase assay was carried out by Nanjing Anakang Biotechnology Co., Ltd. The experimental method followed the report in another part of our work.<sup>29</sup> Reagents: human recombination MAP3K14 protein (Carna, catalog no. 07-102), NIK ADP-Glo assay kit (Promega, catalog no. V9101). The assay was performed in two steps: (1). Terminate the kinase reaction with an equal volume of ADP-Glo reagent and deplete the excess ATP. (2). Convert ADP to ATP with kinase detection reagent, and then use luciferase/luciferin reaction to measure the newly generated ATP. The Preparation of buffer solution: (a) General biochemical reaction buffer: 100  $\mu$ M  $\text{Na}_3\text{VO}_4$ , 2 mM DTT, 0.02 mg/mL BSA, 2 mM  $\text{MgCl}_2$ , Tris pH 7.5, 5% DMSO. (b) 2.5  $\times$  NIK (5 nM) biochemical analysis buffer. (c) 25  $\mu$ M 2.5  $\times$  ATP assay buffer. 1.0  $\mu$ L DMSO solution (5%) of the compounds were added to a specific well (96-well plate). Buffer was added to the positive and negative control wells. 2  $\mu$ L 2.5  $\times$  NIK and 4  $\mu$ L 2.5  $\times$  ATP was added to both compounds and the positive control wells. Besides, for negative control wells, 2  $\mu$ L 2.5  $\times$  ATP and 2  $\mu$ L assay buffer were added. The reaction mixture was incubated for 120 min at room temperature. After the incubation was completed, 5  $\mu$ L ADP-Glo reagent was added to each well, and the plate was incubated for another 40 min. Subsequently, 10  $\mu$ L of detection reagent was added to each well, and their luminescence intensity was measured after 40 min of incubation. According to the conversion curve of ATP to ADP, the luminous intensity is converted into ADP concentration. The  $\text{IC}_{50}$  value was calculated by Prism (GraphPad software) curve fitting.

### **Griess Reagent Method to Measure the Release of Nitric Oxide from LPS-Induced J774 Macrophages**

The macrophages (extracted from mouse abdominal cavity) were inoculated in a 96-well plate (200  $\mu$ L, concentration:  $2 \times 10^4$  cell/mL), and the medium was (5% bovine fetal serum, 1% penicillin-streptomycin, 1% non-essential amino acids, 2% L-glutamine). The plate was incubated at 37  $^\circ\text{C}$  and 5%  $\text{CO}_2$  for 24 h. The original medium was removed, and replaced with the medium 1640 (197  $\mu$ L/well). DMSO solution of the test

compounds (1  $\mu\text{M}$  concentration, 3 replicate wells/sample), 2  $\mu\text{L}$  DMSO and 2  $\mu\text{L}$  medium were added to the drug group, model group, and blank group, respectively. The well plate was placed in a 5%  $\text{CO}_2$ , 37  $^\circ\text{C}$  incubator for 2.0 h. A LPS (200  $\mu\text{g}/\text{mL}$ ) mixture with 1  $\mu\text{L}$  PBS was added to the control and test groups (final concentration is 1  $\mu\text{g}/\text{mL}$ ). After culturing for 22 hours, 100  $\mu\text{L}$  of supernatant from each well was transferred to a new 96-well plate. Subsequently, 100  $\mu\text{L}$  of Griess reagent (1% sulfonamide, 0.1% naphthalenediamine dihydrochloride, and 2.5% phosphoric acid) was added to each supernatant. Make a standard curve (double-diluted sodium nitrite solution, initial concentration: 200  $\mu\text{mol}/\text{L}$ , serial dilution eleven times), and use a microplate reader to read. Linear regression assay was used to determine the concentration of NO in the supernatant (under 540 nm).

#### **Anti-Proliferative Activity of Selected Compounds against Splenic T cells Stimulated by Con A**

Primary T cells were isolated from spleen tissue (EasySep<sup>TM</sup> Mouse T Cell Isolation Kit, Stemcell Technologies, catalog number: 19851). Primary T cells were suspended in RPMI (1% penicillin/streptomycin, 2% glutamine) medium diluted in 10% PBS. Subsequently, it was seeded in a 96-well culture plate (cell density:  $2 \times 10^6$  cells/mL per well). The drug group was added with 2  $\mu\text{M}$  or 0.4  $\mu\text{M}$  NIK inhibitors (3 replicate wells for each sample), while the blank control group was added with the same amount of DMSO. After the addition, Con A (Sigma, 5  $\mu\text{g}/\text{mL}$ ) was used to induce T cell proliferation, and then incubated the plate at 37  $^\circ\text{C}$ , 5%  $\text{CO}_2$  for 48 h. According to the operating manual (CCK8 assay, MedChemExpress) provided by the manufacturer, the compound's anti-Con A-dependent T cell proliferation activity was determined.

#### **Pharmacokinetic Evaluation of Compound 24c**

**Metabolic Stability Assay in Liver Microsomes:** The multi-species liver microsomal metabolic stability assay was based on the test method described by 3D BioOptima Co. Ltd. The types of liver microsomes include rat liver microsomes (RLM), canine liver microsomes (DLM), monkey liver microsomes (CLM), and human liver microsomes (HLM). To each well labeled (T0, T5, T15, T30, T60, NCF60), test compound or control drug solution was added. Subsequently, the mixture of the microsome solution (80  $\mu\text{L}/\text{well}$ ) and the test compound was incubated at 37 $^\circ\text{C}$  for 10 min. 10  $\mu\text{L}$  of 100 mM potassium phosphate buffer was added to the designated wells

(NCF60), after the addition, incubate for 1.0 h at 37 °C. A mixture of tolbutamide and labetalol (1:1) was used to stop the reaction at 5 (T5 wells), 15 (T15 wells), 30 (T30 wells), and 60 (T60 wells) minutes after incubation. The mixture was vortexed for 5 minutes, centrifuged at 4000 rpm at 4 °C for 20 min, and LC-MS analyzed the remaining compound in the supernatant. The data was analyzed through first-order kinetics to calculate " $T_{1/2}$ " and "CL".

**Determination of Pharmacokinetic (PK) Parameters in SD Rats:** Six 8-week-old male Sprague-Dawley mice were fasted overnight and used for pharmacokinetic studies under the intravenous or oral administration routes. The doses of 1.0 and 10 mg/kg were administered via a single intravenous (IV) rapid bolus and intragastric administration. Compound **24c** was suspended in physiological saline containing 0.5% Carboxymethyl cellulose sodium salt(CMC-Na) and 0.2% Tween 80 to prepare an oral prescription (1.0 mg/mL). Processing of the collected plasma samples: the samples were divided into 30  $\mu$ L aliquots, and Acetonitrile (150  $\mu$ L) containing 5 ng/mL verapamil and 50 ng/mL glibenclamide was added to each aliquot for protein precipitation. The mixture was vortexed for 10 min and centrifuged at 3700 rpm for 10 min. An equal volume of water was added to the separated supernatant (70  $\mu$ L), and the mixture was vortexed for 10 minutes. Subsequently, 15  $\mu$ L mixture was injected into the LC/MS system and analyzed using Agilent Technologies 6430.

### Molecular Modeling

The X-ray co-crystal structure of the NIK protein binding with corresponding small molecules was retrieved from the Protein Data Bank<sup>36</sup> (PDB codes: 4G3E). Following the pre-processing wizard (Ligand Preparation module) in Maestro (Schrodinger 2018), the conformational optimization of the target compound is implemented under standard settings. According to the standard procedure suggested by the protein preparation (Protein Preparation module), the NIK protein was pre-processed, and the grid file was generated (using Receptor Grid Generation, version 11.5). In the standard and ultra-precision modes, the binding conformation of the ligand and NIK protein is obtained (the docking is set according to the Glide standard). Among them, only the docking results with low energy configuration and good hydrogen bond geometry trends are considered. Finally, HprSnap 7 is used to edit pictures.

## General Procedures.

Unless otherwise specified, all reagents were purchased from suppliers. Commercially available chemically pure (CP, Chemically Pure) or analytical pure (AR, Analytical Reagent) reagent products were used without further purification. The products were purified by pressurized fast column chromatography, and the stationary phase is usually 100-200 mesh or 200-300 mesh silica gel produced by Qingdao Ocean Chemical Factory. The melting points were determined by an X-4 digital-display micro melting-point apparatus (Beijing Tech Instrument Company, Ltd., Beijing, China). The NMR spectrums were recorded on the Bruker AVANCE AV-600 spectrometer (400 or 300 MHz for  $^1\text{H}$ , 100 or 75 MHz for  $^{13}\text{C}$ ). The chemical shift ( $\delta$ ) and coupling constants ( $J$ ) are reported in ppm and Hz, respectively, and the solvent signal is used as a reference. Mass spectrometry data were obtained on Agilent 1100 LC / MSD mass spectrometer (Agilent, USA) and Q-tofmicro MS (micromass company). All reactions were monitored by TLC (Merck Kieselgel GF254), and spots were visualized with UV light or iodine. HPLC conditions: chromatographic column used C18 (1.8  $\mu\text{M}$ , 4.6 mm  $\times$  30 mm, Agilent), mobile phase A was methanol (chromatographic grade), mobile phase B was purified water (wahaha brand); isocratic elution, methanol: water = 80: 20, the column temperature was 35  $^\circ\text{C}$ , the fluorescence detector was 365 and 220 nm. The compound used for biological evaluation (HPLC analysis) shall have a purity of not less than 95%.

**The Preparation of 7-nitronaphthalene-1,3-diol (compound 10) was in accordance with relevant known literature .<sup>37</sup>**

### The Preparation of 2,4-Dibromo-6-nitroquinoline (11)

To a toluene (100 mL) solution of compound **10** (1.05 g, 5.09 mmol),  $\text{POBr}_3$  (4.38 g, 15.3 mmol) was added under  $\text{N}_2$  atmosphere and room temperature. After the addition, the reaction mixture was moved to 110  $^\circ\text{C}$  oil bath and stirred for 2 h. After the reaction was completed, the reaction was naturally cooled to room temperature. The mixture was extracted with EA (50 mL  $\times$  3), combined organic phase, and concentrated under vacuum. The residue was chromatographed, eluting with a gradient (PE / EA = 30: 1) to afford title compound **11** (1.38 g, yield 82%) as a white solid. ESI-MS  $m/z$   $[\text{M} + \text{H}]^+$ : 332.7.  $^1\text{H}$  NMR (300 MHz,  $\text{CDCl}_3$ )  $\delta$  9.11 (s, 1H), 8.55 (d,  $J = 9.1$  Hz, 1H), 8.19 (d,  $J = 9.1$  Hz, 1H), 8.01 (s, 1H).

### The Preparation of 4-bromo-6-nitroquinolin-2-ol (**12**)

In a 100 mL reaction flask, 2,4-dibromo-6-nitroquinoline (1.34 g, 4.05 mmol) was added and then dissolved in acetic acid (25 mL). The reaction was heated at 90 °C and stirred overnight. The reaction mixture was slowly poured into an ice-water mixture, and a large amount of white solid precipitated out. The suspension was filtered, then filter cake was transferred, and vacuum dried to afford the title compound **12** (1.03 g, 95%) as a white solid. ESI-MS  $m/z$   $[M + H]^+$ : 270.1.  $^1\text{H NMR}$  (300 MHz,  $\text{DMSO-}d_6$ )  $\delta$  12.57 (s, 1H), 8.57 (d,  $J = 2.5$  Hz, 1H), 8.41 (dd,  $J = 9.1, 2.5$  Hz, 1H), 7.49 (d,  $J = 9.1$  Hz, 1H), 7.23 (d,  $J = 1.7$  Hz, 1H).

### General Procedure A for the Synthesis of Compounds **13b**—**13f**.

**Method A-I:** To a solution of compound **11** (1.2 g, 3.62 mmol) in DMF, appropriate primary or secondary amines in DMF (1.0 mL) were added dropwise at 0 °C, under  $\text{N}_2$  atmosphere. Subsequently,  $\text{Et}_3\text{N}$  (1.5 mL, 10.86 mmol) diluted with DMF (1.0 mL) was added in the same way. After the addition was completed, the mixture was continuously stirred at this temperature for 2 h. The reaction mixture was concentrated under vacuum. The residue was chromatographed, eluting with a gradient (DCM / MeOH = 40: 1) to afford title compound **13b**—**13d**, **13f** (yield, 64%-88%).

**Method A-II:** Compound **12** (1.08 g, 4.00 mmol) was dissolved in DCM (60 mL), and stirred vigorously under  $\text{N}_2$  atmosphere at 0 °C. NaH (60%, 480 mg) was added in batches within 5 min, and then stirred for 30 min after the addition. 1-(2-bromoethyl)piperidine (1.66 mL, 12 mmol) was added dropwise. The reaction mixture was naturally warmed to room temperature and stirred overnight. After the reaction was complete, the mixture was slowly poured into ice water to quench the excess NaH. The mixture was extracted with EA (60 mL  $\times$  3). The combined organic layers were washed with brine, dried over  $\text{Na}_2\text{SO}_4$ , and concentrated under vacuum. The residue was chromatographed, eluting with a gradient (PE / EA = 20 : 1) to afford title compound **13e** (924mg, 60%) as a yellow solid. ESI-MS  $m/z$   $[M + H]^+$ : 383.2.  $^1\text{H NMR}$  (400 MHz,  $\text{DMSO-}d_6$ )  $\delta$  8.40 (s, 1H), 8.35 – 8.28 (m, 2H), 7.63 (s, 1H), 4.63 (d,  $J = 7.5$  Hz, 2H), 3.61 (s, 4H), 3.23 – 3.18 (m, 2H), 2.77 (s, 4H).

**4-bromo-N-methyl-6-nitroquinolin-2-amine (13b).** Compound **13b** was prepared according to general procedure A-I on a 3.0 mmol scale. Purification by column chromatography (2.5% MeOH / DCM) afforded the

title compound (638.4 mg, 2.26 mmol, 75% yield).  $[M + H]^+$ : 283.1.  $^1\text{H NMR}$  (300 MHz,  $\text{DMSO-}d_6$ )  $\delta$  8.62 (d,  $J = 2.6$  Hz, 1H), 8.26 (dd,  $J = 9.2, 2.7$  Hz, 1H), 7.99 – 7.85 (m, 1H), 7.61 (d,  $J = 9.1$  Hz, 1H), 7.29 (s, 1H), 2.95 (d,  $J = 4.7$  Hz, 3H).

**4-bromo-N-(2-methoxyethyl)-N-methyl-6-nitroquinolin-2-amine (13c)** Compound **13c** was prepared according to general procedure A-I on a 4.0 mmol scale. Purification by column chromatography (2.5% MeOH / DCM) afforded the title compound (1.2 g, 3.53 mmol, 88% yield).  $[M + H]^+$ : 341.1.  $^1\text{H NMR}$  (300 MHz,  $\text{DMSO-}d_6$ )  $\delta$  8.63 (d,  $J = 2.6$  Hz, 1H), 8.25 (dd,  $J = 9.2, 2.7$  Hz, 1H), 7.66 (s, 1H), 7.58 (d,  $J = 9.2$  Hz, 1H), 3.94 – 3.88 (m, 2H), 3.59 (t,  $J = 5.4$  Hz, 2H), 3.27 (s, 3H), 3.22 (s, 3H).

**$\text{N}^1$ -(4-bromo-6-nitroquinolin-2-yl)- $\text{N}^1, \text{N}^2, \text{N}^2$ -trimethylethane-1,2-diamine (13d)** Compound **13d** was prepared according to general procedure A-I on a 3.85 mmol scale. Purification by column chromatography (3% MeOH / DCM) afforded the title compound (868.8 g, 2.46 mmol, 64% yield).  $[M + H]^+$ : 354.2.  $^1\text{H NMR}$  (300 MHz,  $\text{CDCl}_3$ )  $\delta$  8.80 (d,  $J = 3.0$  Hz, 1H), 8.22 (dd,  $J = 9.0, 3.0$  Hz, 1H), 7.56 (d,  $J = 9.0$  Hz, 1H), 7.21 (s, 1H), 3.78 (t,  $J = 7.5$  Hz, 2H), 3.17 (s, 3H), 2.53 (t,  $J = 7.5$  Hz, 2H), 2.28 (s, 6H).

**4-bromo-2-(4-methylpiperazin-1-yl)-6-nitroquinoline (13f)** Compound **13f** was prepared according to general procedure A-I on a 2.4 mmol scale. Purification by column chromatography (3% MeOH / DCM) afforded the title compound (648.5 g, 1.84 mmol, 77% yield).  $[M + H]^+$ : 352.3.  $^1\text{H NMR}$  (300 MHz,  $\text{DMSO-}d_6$ )  $\delta$  8.64 (d,  $J = 2.6$  Hz, 1H), 8.27 (dd,  $J = 9.2, 2.7$  Hz, 1H), 7.84 (s, 1H), 7.60 (d,  $J = 9.2$  Hz, 1H), 3.81 (t,  $J = 5.0$  Hz, 4H), 2.42 (t,  $J = 5.0$  Hz, 4H), 2.23 (s, 3H).

### General Procedure B for the Synthesis of Compounds 14a—14f.

Starting materials **13a — 13f** (2 mmol, 1.0 equiv), tert-butyl 4-(4,4,5,5-tetramethyl-1,3,2-dioxaborolan-2-yl)-1H-pyrazole-1-carboxylate (1.76 g, 6.0 mmol),  $\text{PdCl}_2(\text{dppf})$  (73.2 mg, 5% mmol), X-Phos (95.2 mg, 10% mmol),  $\text{K}_2\text{CO}_3$  (829.2 mmol, 6 mmol) were suspended in 24 mL dioxane / water (6 : 1), and stirred at 80 °C for 4.0 h under  $\text{N}_2$  atmosphere. After completion of reaction, The mixture was extracted with EA (60 mL  $\times$  3), resulting organic layers, which were concentrated under vacuum. The crude product was then transferred to a 50 mL reaction flask and dissolved in 20 mL DCM.  $\text{CF}_3\text{COOH}$  (0.37 mL, 5.0 mmol) was added dropwise to the reaction

mixture at room temperature, and after the addition, the mixture was stirred overnight. After the “-Boc” protecting group was completely removed, the reaction mixture was poured into ice water.  $K_2CO_3$  was used to neutralize excess  $CF_3COOH$ . The mixture was extracted with EA (60 mL  $\times$  3). The combined organic layers were washed with brine, dried over  $Na_2SO_4$ , and concentrated under vacuum. The residue was chromatographed, eluting with a gradient of (DCM / MeOH = 30: 1) to afford title compounds **14a** — **14f** ( yield, 65%-86%) as a yellow solid.

**6-nitro-4-(1H-pyrazol-4-yl)quinolin-2-ol (14a).** Compound **14a** was prepared according to general procedure B on a 4.46 mmol scale. Purification by column chromatography (3% MeOH / DCM) afforded the title compound (740.0 mg, 2.89 mmol, 65% yield).  $[M + Na]^+$ : 279.1.  $^1H$  NMR (300 MHz,  $DMSO-d_6$ )  $\delta$  13.44 (s, 1H), 12.31 (s, 1H), 8.63 (d,  $J = 2.5$  Hz, 1H), 8.38 (dd,  $J = 9.1, 2.5$  Hz, 2H), 7.98 (s, 1H), 7.51 (d,  $J = 9.1$  Hz, 1H), 6.68 (d,  $J = 1.2$  Hz, 1H).

**N-methyl-6-nitro-4-(1H-pyrazol-4-yl)quinolin-2-amine (14b).** Compound **14b** was prepared according to general procedure B on a 2.0 mmol scale. Purification by column chromatography (4% MeOH / DCM) afforded the title compound (463.0 mg, 1.72 mmol, 86% yield).  $[M + H]^+$ : 270.2.  $^1H$  NMR (300 MHz,  $DMSO-d_6$ )  $\delta$  13.38 (s, 1H), 8.68 (d,  $J = 2.7$  Hz, 1H), 8.24 (dd,  $J = 9.0, 2.7$  Hz, 2H), 7.90 (s, 1H), 7.74 – 7.71 (m, 1H), 7.63 (d,  $J = 9.2$  Hz, 1H), 6.86 (s, 1H), 2.98 (d,  $J = 6.0$  Hz, 3H).

**N-(2-methoxyethyl)-N-methyl-6-nitro-4-(1H-pyrazol-4-yl)quinolin-2-amine (14c).** Compound **14c** was prepared according to general procedure B on a 3.55 mmol scale. Purification by column chromatography (4% MeOH / DCM) afforded the title compound (880.2 mg, 2.69 mmol, 76 % yield).  $[M + H]^+$ : 328.3.  $^1H$  NMR (300 MHz,  $DMSO-d_6$ )  $\delta$  13.40 (s, 1H), 8.81 – 8.65 (m, 1H), 8.34 (d,  $J = 6.5$  Hz, 1H), 8.24 (d,  $J = 8.5$  Hz, 1H), 7.98 (d,  $J = 6.4$  Hz, 1H), 7.63 (d,  $J = 8.2$  Hz, 1H), 7.16 (t,  $J = 5.0$  Hz, 1H), 3.92 (s, 2H), 3.60 (t,  $J = 5.2$  Hz, 2H), 3.33 – 3.24 (m, 6H).

**$N^1, N^1, N^2$ -trimethyl- $N^2$ -(6-nitro-4-(1H-pyrazol-4-yl)quinolin-2-yl)ethane-1,2-diamine (14d).** Compound **14d** was prepared according to general procedure B on a 2.46 mmol scale. Purification by column chromatography (9% MeOH / DCM) afforded the title compound (556.1 mg, 1.63 mmol, 66 % yield).  $[M + H]^+$ : 341.4.  $^1H$  NMR

(300 MHz, DMSO- $d_6$ )  $\delta$  13.39 (s, 1H), 8.74 (d,  $J$  = 2.6 Hz, 1H), 8.26 – 8.22 (m, 3H), 7.61 (d,  $J$  = 9.2 Hz, 1H), 7.13 (s, 1H), 3.86 (t,  $J$  = 6.5 Hz, 2H), 3.36 (s, 3H), 2.56 (t,  $J$  = 6.7 Hz, 2H), 2.25 (s, 6H).

**4-(2-((6-nitro-4-(1H-pyrazol-4-yl)quinolin-2-yl)oxy)ethyl)morpholine (14e).** Compound **14e** was prepared according to general procedure B on a 2.85 mmol scale. Purification by column chromatography (4% MeOH / DCM) afforded the title compound (860.4 mg, 2.32 mmol, 82 % yield).  $[M + H]^+$ : 370.3.  $^1H$  NMR (400 MHz, DMSO- $d_6$ )  $\delta$  13.37 (s, 1H), 8.63 (s, 2H), 8.31 (s, 1H), 7.95 – 7.87 (m, 2H), 7.43 (s, 1H), 4.40 (d,  $J$  = 7.7 Hz, 2H), 3.58 (s, 4H), 3.10 – 3.08 (m, 1H), 2.58 (s, 4H), 1.20 (t,  $J$  = 7.4 Hz, 1H).

**2-(4-methylpiperazin-1-yl)-6-nitro-4-(1H-pyrazol-4-yl)quinoline (14f).** Compound **14f** was prepared according to general procedure B on a 2.0 mmol scale. Purification by column chromatography (4% MeOH / DCM) afforded the title compound (493.8 mg, 1.46 mmol, 73 % yield).  $[M + H]^+$ : 339.3.  $^1H$  NMR (300 MHz, DMSO- $d_6$ )  $\delta$  13.39 (s, 1H), 8.75 (d,  $J$  = 2.6 Hz, 1H), 8.36 (s, 1H), 8.26 (dd,  $J$  = 9.2, 2.7 Hz, 1H), 8.01 (s, 1H), 7.65 (d,  $J$  = 9.2 Hz, 1H), 7.34 (s, 1H), 3.88 – 3.84 (m, 4H), 2.49 – 2.45 (m, 4H), 2.26 (s, 3H).

### General Procedure C for the Synthesis of Compounds 15a—15f.

To a solution of 6-nitro-4-(1H-pyrazol-4-yl) quinoline derivatives **14a—14f** (1.4 mmol) in ethanol (9.6 mL) and water (3.2 mL), Fe (783 mg, 14 mmol) and  $NH_4Cl$  (748.8 mg, 14 mmol). After the reaction was refluxed at 90°C for 1.0 h, the reaction mixture was filtered through celite and the filter cake was washed with MeOH. The filtrate was concentrated under vacuum, the resulting residue was extracted with EA (60 mL  $\times$  3), and the organic phases were combined, dried over  $Na_2SO_4$ , and concentrated in vacuo to afford corresponding crude 4-(1H-pyrazol-4-yl)quinolin-6-amine derivatives **15a—15f**, which were used without further purification.

### General Procedure D for the Synthesis of Compounds 16a—16f.

To the  $CH_3CN$  (3.0 mL) solution of compounds **15a—15f** (1.0 mmol) was added p-toluenesulfonic acid (516.6 mg, 3.0 mmol) to obtain a suspension. After cooling to 0 °C, an aqueous solution (0.73 mL) of sodium nitrite (138.0 mg, 2.0 mmol) and KI (414.9 mg, 2.5 mmol) was slowly added dropwise to the reaction system (during dropping process, the reaction temperature was controlled below 5°C). After the addition, the reaction mixture was naturally warmed to room temperature and stirred for 2.0 hours. The reaction solution was

quenched with an aqueous solution of  $\text{Na}_2\text{S}_2\text{O}_3$  (4.0 mL). The mixture was extracted with  $\text{CH}_2\text{Cl}_2$  (50 mL  $\times$  3). The combined organic layer was washed with brine, dried over  $\text{Na}_2\text{SO}_4$  and concentrated under vacuum. The residue was chromatographed, eluting with a gradient of (DCM / MeOH = 30: 1) to afford title compounds **14a** – **14f** ( yield, 46%-82%) as a yellow solid.

**6-iodo-4-(1H-pyrazol-4-yl)quinolin-2-ol (16a)**. Compound **16a** was prepared according to general procedure D on a 1.0 mmol scale. Purification by column chromatography (4% MeOH / DCM) afforded the title compound (209.0 mg, 0.62 mmol, 62 % yield).  $[\text{M} + \text{H}]^+$ : 338.2.  $^1\text{H}$  NMR (300 MHz,  $\text{DMSO}-d_6$ )  $\delta$  13.33 (s, 1H), 11.84 (s, 1H), 8.02 (d,  $J = 1.9$  Hz, 3H), 7.83 (dd,  $J = 8.6, 1.9$  Hz, 1H), 7.19 (d,  $J = 8.6$  Hz, 1H), 6.51 (s, 1H).

**6-iodo-N-methyl-4-(1H-pyrazol-4-yl)quinolin-2-amine (16b)**. Compound **16b** was prepared according to general procedure D on a 1.0 mmol scale. Purification by column chromatography (4% MeOH / DCM) afforded the title compound (198.5 mg, 0.57 mmol, 57 % yield).  $[\text{M} + \text{Na}]^+$ : 373.1.  $^1\text{H}$  NMR (300 MHz,  $\text{DMSO}-d_6$ )  $\delta$  13.26 (s, 1H), 8.17 (s, 1H), 8.06 (d,  $J = 2.1$  Hz, 1H), 7.79 (s, 1H), 7.72 (dd,  $J = 8.7, 2.1$  Hz, 1H), 7.36 (d,  $J = 8.7$  Hz, 1H), 7.13 (s, 1H), 6.71 (s, 1H), 2.91 (d,  $J = 4.6$  Hz, 3H).

**6-iodo-N-(2-methoxyethyl)-N-methyl-4-(1H-pyrazol-4-yl)quinolin-2-amine (16c)**. Compound **16c** was prepared according to general procedure D on a 1.0 mmol scale. Purification by column chromatography (4% MeOH / DCM) afforded the title compound (332.7 mg, 0.82 mmol, 82 % yield).  $[\text{M} + \text{H}]^+$ : 409.3.  $^1\text{H}$  NMR (300 MHz,  $\text{CDCl}_3$ )  $\delta$  8.07 (d,  $J = 2.0$  Hz, 1H), 7.81 (s, 2H), 7.67 (dd,  $J = 8.8, 2.0$  Hz, 1H), 7.44 – 7.41 (m, 1H), 6.78 (s, 1H), 3.83 (t,  $J = 6.0$  Hz, 2H), 3.60 (t,  $J = 6.0$  Hz, 2H), 3.30 (s, 3H), 3.19 (s, 3H).

**$\text{N}^1$ -(6-iodo-4-(1H-pyrazol-4-yl)quinolin-2-yl)- $\text{N}^1, \text{N}^2, \text{N}^2$ -trimethylethane-1,2-diamine (16d)**. Compound **16d** was prepared according to general procedure D on a 1.0 mmol scale. Purification by column chromatography (8% MeOH / DCM) afforded the title compound (267.6 mg, 0.64 mmol, 64 % yield).  $[\text{M} + \text{H}]^+$ : 422.1.  $^1\text{H}$  NMR (300 MHz,  $\text{DMSO}-d_6$ )  $\delta$  13.31 (s, 1H), 8.19– 8.12(m, 3H), 7.82 – 7.78 (m, 1H), 7.43 (d,  $J = 8.8$  Hz, 1H), 7.05 (s, 1H), 4.06 (d,  $J = 6.2$  Hz, 2H), 3.38 (d,  $J = 6.1$  Hz, 2H), 3.18 (s, 3H), 2.92 (s, 6H).

**4-(2-((6-iodo-4-(1H-pyrazol-4-yl)quinolin-2-yl)oxy)ethyl)morpholine (16e)**. Compound **16e** was prepared according to general procedure D on a 1.0 mmol scale. Purification by column chromatography (7% MeOH /

DCM) afforded the title compound (274.8 mg, 0.61 mmol, 61 % yield).  $[M + H]^+$ : 451.2.  $^1\text{H NMR}$  (300 MHz,  $\text{DMSO-}d_6$ )  $\delta$  13.36 (s, 1H), 8.26 (s, 1H), 8.09 (d,  $J = 2.1$  Hz, 1H), 7.96 – 7.84 (m, 2H), 7.45 (d,  $J = 9.0$  Hz, 1H), 6.62 (s, 1H), 4.38 (t,  $J = 7.1$  Hz, 2H), 3.56 (t,  $J = 4.6$  Hz, 4H), , 3.37 (s, 4H) , 2.56 (d,  $J = 7.1$  Hz, 2H).

**6-iodo-2-(4-methylpiperazin-1-yl)-4-(1H-pyrazol-4-yl)quinoline (16f)**. Compound **16f** was prepared according to general procedure D on a 1.0 mmol scale. Purification by column chromatography (8% MeOH / DCM) afforded the title compound (193.7 mg, 0.46 mmol, 46 % yield).  $[M + H]^+$ : 420.2.  $^1\text{H NMR}$  (300 MHz,  $\text{DMSO-}d_6$ )  $\delta$  13.30 (s, 1H), 8.16 (d,  $J = 3.0$  Hz, 3H), 7.77 (dd,  $J = 9.0, 3.0$  Hz, 1H), 7.39 (d,  $J = 9.0$  Hz, 1H), 7.18 (s, 1H), 3.72 (t,  $J = 4.5$  Hz, 4H), 2.43 (t,  $J = 4.5$  Hz, 4H), 2.23 (s, 3H).

### General Procedure E for the Synthesis of Compounds **17a**—**17f**.

To a suspension containing **16e**—**16f** (1.0 equiv),  $\text{PdCl}_2(\text{PPh}_3)_2$  (5% mmol), CuI (10% mmol) in THF /  $\text{Et}_3\text{N}$  = 3: 1 (total concentration: 0.2 M), the corresponding terminal alkynes in THF (1 mL) was added dropwise. In some cases, anhydrous DMF (2 mL) was added to the reaction system to keep the starting materials completely dissolved. After the reaction was completed, the mixture was evaporated in vacuo. The residue was chromatographed, eluting with a gradient of (DCM / MeOH = 15: 1) to afford title compounds **17a** — **17f** ( yield,31%-54%) as a yellow solid.

**6-(3-hydroxy-3-(thiazol-2-yl)but-1-yn-1-yl)-4-(1H-pyrazol-4-yl)quinolin-2-ol (17a)**. Compound **17a** was prepared according to general procedure E on a 0.4 mmol scale. Purification by column chromatography (4% MeOH / DCM) afforded the title compound (52.1 mg, 0.14 mmol, 36% yield). White solid; mp 285-287 °C. HPLC analysis: retention time, 2.978 min; peak area, 98.46%.  $^1\text{H NMR}$  (400 MHz,  $\text{DMSO-}d_6$ )  $\delta$  13.34 (s, 1H), 11.93 (s, 1H), 8.96 (s, 1H), 8.24 (s, 1H), 7.87 (s, 1H), 7.76 – 7.66 (m, 2H), 7.56 (dd,  $J = 8.5, 1.9$  Hz, 1H), 7.36 (d,  $J = 8.5$  Hz, 1H), 7.02 (s, 1H), 6.52 (s, 1H), 1.85 (s, 3H);  $^{13}\text{C NMR}$  (100 MHz,  $\text{DMSO-}d_6$ )  $\delta$  176.43, 161.80, 143.19, 143.01, 139.81, 133.62, 129.41, 121.06, 120.90, 118.74, 116.80, 116.34, 115.47, 92.19, 83.14, 68.34, 31.97. ESI-MS  $m/z$ : 363.2  $[M + H]^+$ .

**4-(2-(methylamino)-4-(1H-pyrazol-4-yl)quinolin-6-yl)-2-(thiazol-2-yl)but-3-yn-2-ol (17b)**. Compound **17b** was prepared according to general procedure E on a 0.4 mmol scale. Purification by column chromatography (5%

MeOH / DCM) afforded the title compound (61.2 mg, 0.16 mmol, 41% yield). White solid; mp 218-221 °C. HPLC analysis: retention time, 3.544 min; peak area, 99.69%. <sup>1</sup>H NMR (600 MHz, DMSO-*d*<sub>6</sub>) δ 13.27 (s, 1H), 8.17 (s, 1H), 7.79 (dd, *J* = 20.5, 2.6 Hz, 3H), 7.67 (d, *J* = 3.3 Hz, 1H), 7.52 (d, *J* = 8.6 Hz, 1H), 7.45 (dd, *J* = 8.6, 1.9 Hz, 1H), 7.20 (q, *J* = 3.9 Hz, 1H), 6.99 (s, 1H), 6.73 (s, 1H), 2.92 (d, *J* = 4.7 Hz, 3H), 1.87 (s, 3H); <sup>13</sup>C NMR (100 MHz, DMSO-*d*<sub>6</sub>) δ 176.64, 158.32, 158.25, 149.12, 143.00, 139.49, 131.95, 128.91, 126.88, 121.85, 120.86, 117.30, 117.26, 114.47, 113.03, 91.94, 84.17, 68.38, 32.03, 28.05. ESI-MS *m/z*: 376.3 [M + H]<sup>+</sup>.

**4-(2-((2-methoxyethyl)(methyl)amino)-4-(1*H*-pyrazol-4-yl)quinolin-6-yl)-2-(thiazol-2-yl)but-3-yn-2-ol (17c).**

Compound **17c** was prepared according to general procedure E on a 0.4 mmol scale. Purification by column chromatography (5% MeOH / DCM) afforded the title compound (54.2 mg, 0.12 mmol, 31% yield). White solid; mp 138-140 °C. HPLC analysis: retention time, 3.807 min; peak area, 98.25%. <sup>1</sup>H NMR (400 MHz, DMSO-*d*<sub>6</sub>) δ 13.28 (s, 1H), 8.08 – 7.88 (m, 3H), 7.78 (d, *J* = 3.2 Hz, 1H), 7.68 (d, *J* = 3.2 Hz, 1H), 7.56 – 7.47 (m, 2H), 7.02 (d, *J* = 7.2 Hz, 2H), 3.86 (t, *J* = 4.0 Hz, 2H), 3.57 (t, *J* = 6.0 Hz, 2H), 3.27 (s, 3H), 3.19 (s, 3H), 1.86 (s, 3H); <sup>13</sup>C NMR (100 MHz, DMSO-*d*<sub>6</sub>) δ 176.60, 157.24, 143.00, 140.50, 132.09, 128.89, 127.20, 121.01, 120.86, 117.74, 114.68, 109.69, 92.08, 84.16, 79.64, 70.44, 68.38, 58.67, 49.23, 37.22, 32.02. ESI-MS *m/z*: 434.4 [M + H]<sup>+</sup>.

**4-(2-((2-(dimethylamino)ethyl)(methyl)amino)-4-(1*H*-pyrazol-4-yl)quinolin-6-yl)-2-(thiazol-2-yl)but-3-yn-2-ol (17d).**

Compound **17d** was prepared according to general procedure E on a 0.2 mmol scale. Purification by column chromatography (8% MeOH / DCM) afforded the title compound (43.8 mg, 0.1 mmol, 49% yield). White solid; mp 177-179 °C. HPLC analysis: retention time, 4.228 min; peak area, 96.72%. <sup>1</sup>H NMR (300 MHz, DMSO-*d*<sub>6</sub>) δ 11.78 (s, 1H), 8.66 (s, 1H), 8.25 (s, 1H), 7.98 (s, 1H), 7.76 (d, *J* = 3.3 Hz, 1H), 7.67 (d, *J* = 3.2 Hz, 1H), 7.25 – 7.22 (m, 1H), 7.11 (s, 2H), 6.47 (dd, *J* = 3.5, 1.7 Hz, 1H), 3.16 (d, 4H), 2.59 (d, *J* = 5.7 Hz, 4H), 2.26 (s, 3H), 1.86 (s, 3H), 1.83 – 1.77 (m, 2H); <sup>13</sup>C NMR (100 MHz, DMSO-*d*<sub>6</sub>) δ 176.63, 154.20, 151.54, 151.33, 147.72, 142.97, 132.19, 127.83, 127.58, 122.94, 120.85, 120.74, 115.19, 103.82, 98.42, 91.70, 83.80, 68.35, 58.64, 56.99, 54.00, 53.12, 47.00, 32.04, 28.40. ESI-MS *m/z*: 447.6 [M + H]<sup>+</sup>.

**4-(2-(2-morpholinoethoxy)-4-(1*H*-pyrazol-4-yl)quinolin-6-yl)-2-(thiazol-2-yl)but-3-yn-2-ol (17e).**

Compound **17e** was prepared according to general procedure E on a 0.25 mmol scale. Purification by column

chromatography (8% MeOH / DCM) afforded the title compound (46.4 mg, 0.1 mmol, 39% yield). White solid; mp 199-201 °C. HPLC analysis: retention time, 3.508 min; peak area, 96.97%. <sup>1</sup>H NMR (300 MHz, DMSO-*d*<sub>6</sub>) δ 13.36 (s, 1H), 8.08 – 7.83 (m, 3H), 7.78 (d, J = 3.0 Hz, 1H), 7.68 – 7.63 (m, 3H), 7.07 (s, 1H), 6.63 (s, 1H), 4.39 (t, J = 6.0 Hz, 2H), 3.56 (t, J = 4.5 Hz, 4H), 3.37 (s, 4H), 2.57 (d, J = 7.0 Hz, 2H), 1.87 (s, 3H); <sup>13</sup>C NMR (100 MHz, DMSO-*d*<sub>6</sub>) δ 160.88, 142.26, 139.37, 133.84, 129.87, 120.39, 120.13, 116.52, 116.20, 116.11, 96.33, 80.13, 64.10, 55.71, 53.90, 46.01, 32.05, 9.02. ESI-MS *m/z*: 476.5 [M + H]<sup>+</sup>.

**4-(2-(4-methylpiperazin-1-yl)-4-(1*H*-pyrazol-4-yl)quinolin-6-yl)-2-(thiazol-2-yl)but-3-yn-2-ol (17f).** Compound **17f** was prepared according to general procedure E on a 0.2 mmol scale. Purification by column chromatography (8% MeOH / DCM) afforded the title compound (48.1 mg, 0.11 mmol, 54% yield). White solid; mp 138-140 °C. HPLC analysis: retention time, 4.129 min; peak area, 98.51%. <sup>1</sup>H NMR (300 MHz, DMSO-*d*<sub>6</sub>) δ 13.27 (s, 1H), 8.23 (s, 1H), 7.88 (d, J = 3.0 Hz, 2H), 7.76 (d, J = 3.0 Hz, 1H), 7.67 (d, J = 3.0 Hz, 1H), 7.55 (d, J = 9.0 Hz, 1H), 7.50 – 7.47 (m, 1H), 7.19 (s, 1H), 6.99 (s, 1H), 3.73 (s, 4H), 2.42 (s, 4H), 2.23 (s, 3H), 1.87 (s, 3H); <sup>13</sup>C NMR (100 MHz, DMSO-*d*<sub>6</sub>) δ 176.58, 157.67, 148.37, 143.01, 140.85, 132.12, 128.87, 127.50, 121.49, 120.89, 117.63, 115.33, 110.02, 92.29, 84.07, 68.38, 55.00, 46.25, 44.73, 32.01. ESI-MS *m/z*: 445.7 [M + H]<sup>+</sup>. **The preparation of compound 20 was in accordance with relevant known literature<sup>38, 39</sup>.**

**6-nitroquinolin-4-ol (22).** Compound **22** was prepared according to the synthetic method of compound **10** on a 60 mmol scale. Purification by column chromatography (10% EA / PE) afforded the title compound (5.13 g, 27 mmol, 45% yield). [M + H]<sup>+</sup>: 191.0. <sup>1</sup>H NMR (400 MHz, DMSO-*d*<sub>6</sub>) δ 12.29 (s, 1H), 8.84 (d, J = 2.6 Hz, 1H), 8.42 (dd, J = 9.2, 2.7 Hz, 1H), 8.05 (d, J = 4.7 Hz, 1H), 7.73 (d, J = 9.2 Hz, 1H), 6.20 (d, J = 4.7 Hz, 1H).

**6-iodo-4-(1*H*-pyrazol-4-yl)quinoline (23).** Compound **23** was prepared according to the synthetic method of compound **16** on a 4.0 mmol scale. Purification by column chromatography (6% MeOH / DCM) afforded the title compound (899.1 mg, 2.8 mmol, 70% yield). [M + H]<sup>+</sup>: 322.1. <sup>1</sup>H NMR (300 MHz, DMSO-*d*<sub>6</sub>) δ 13.40 (s, 1H), 8.89 (d, J = 4.5 Hz, 1H), 8.52 (t, J = 1.5 Hz, 1H), 8.36 (s, 1H), 8.11 – 7.91 (m, 2H), 7.84 (dd, J = 8.8, 1.1 Hz, 1H), 7.55 (d, J = 4.5 Hz, 1H).

**4-(4-(1H-pyrazol-4-yl)quinolin-6-yl)-2-methylbut-3-yn-2-ol (24a).** Compound **24a** was prepared according to general procedure E on a 0.4 mmol scale. Purification by column chromatography (8% MeOH / DCM) afforded the title compound (95.4 mg, 0.34 mmol, 86% yield). White solid; mp 203-205 °C. HPLC analysis: retention time, 3.474 min; peak area, 98.66%. <sup>1</sup>H NMR (400 MHz, DMSO-*d*<sub>6</sub>) δ 13.38 (s, 1H), 8.87 (d, J = 4.5 Hz, 1H), 8.41 – 7.90 (m, 4H), 7.72 (dd, J = 8.6, 1.9 Hz, 1H), 7.55 (d, J = 4.5 Hz, 1H), 5.54 (s, 1H), 1.51 (s, 6H); <sup>13</sup>C NMR (75 MHz, DMSO-*d*<sub>6</sub>) δ 151.19, 147.93, 139.68, 132.09, 130.47, 128.71, 126.21, 121.85, 121.42, 117.07, 97.79, 80.83, 64.17, 31.99. ESI-MS m/z: 278.2 [M + H]<sup>+</sup>.

**4-(4-(1H-pyrazol-4-yl)quinolin-6-yl)-2-(thiophen-2-yl)but-3-yn-2-ol (24b).** Compound **24b** was prepared according to general procedure E on a 0.26 mmol scale. Purification by column chromatography (8% MeOH / DCM) afforded the title compound (47.3 mg, 0.14 mmol, 53% yield). White solid; mp 196-199 °C. HPLC analysis: retention time, 3.845 min; peak area, 99.55%. <sup>1</sup>H NMR (300 MHz, DMSO-*d*<sub>6</sub>) δ 13.41 (s, 1H), 8.89 (d, J = 4.5 Hz, 1H), 8.36 (s, 1H), 8.24 (s, 1H), 8.10 – 7.93 (m, 2H), 7.78 (dd, J = 8.7, 1.8 Hz, 1H), 7.56 (d, J = 4.5 Hz, 1H), 7.45 (dd, J = 5.1, 1.2 Hz, 1H), 7.21 (dd, J = 3.5, 1.1 Hz, 1H), 7.00 (dd, J = 5.0, 3.6 Hz, 1H), 6.61 (d, J = 1.5 Hz, 1H), 1.86 (s, 3H). <sup>13</sup>C NMR (75 MHz, DMSO-*d*<sub>6</sub>) δ 152.10, 151.45, 148.19, 139.69, 131.98, 130.64, 129.02, 127.07, 126.18, 125.36, 123.80, 121.88, 120.84, 117.07, 95.43, 82.83, 66.55, 34.13. ESI-MS m/z: 346.2 [M + H]<sup>+</sup>.

**4-(4-(1H-pyrazol-4-yl)quinolin-6-yl)-2-(thiazol-2-yl)but-3-yn-2-ol (24c).** Compound **24c** was prepared according to general procedure E on a 0.24 mmol scale. Purification by column chromatography (8% MeOH / DCM) afforded the title compound (39.7 mg, 0.11 mmol, 48% yield). White solid; mp 230-233 °C. HPLC analysis: retention time, 3.332 min; peak area, 97.27%. <sup>1</sup>H NMR (300 MHz, DMSO-*d*<sub>6</sub>) δ 13.40 (s, 1H), 8.88 (d, J = 4.5 Hz, 1H), 8.35 (s, 1H), 8.20 (d, J = 1.6 Hz, 1H), 8.04 (d, J = 8.7 Hz, 1H), 7.96 (s, 1H), 7.79 (d, J = 3.2 Hz, 1H), 7.74 (dd, J = 8.7, 1.8 Hz, 1H), 7.70 (d, J = 3.2 Hz, 1H), 7.55 (d, J = 4.5 Hz, 1H), 7.13 (s, 1H), 1.90 (s, 3H); <sup>13</sup>C NMR (75 MHz, DMSO-*d*<sub>6</sub>) δ 176.26, 151.50, 148.19, 143.07, 139.72, 131.90, 130.65, 129.16, 126.15, 121.91, 120.99, 120.54, 117.02, 94.04, 83.35, 68.42, 31.95. ESI-MS m/z: 347.5 [M + H]<sup>+</sup>.

**4-(4-(1H-pyrazol-4-yl)quinolin-6-yl)-2-(pyridin-2-yl)but-3-yn-2-ol (24d).** Compound **24d** was prepared according to general procedure E on a 0.20 mmol scale. Purification by column chromatography (8% MeOH /

DCM) afforded the title compound (28.4 mg, 0.08 mmol, 42% yield). White solid; mp 170-173 °C. HPLC analysis: retention time, 3.423 min; peak area, 95.07%. <sup>1</sup>H NMR (300 MHz, DMSO-*d*<sub>6</sub>) δ 13.39 (s, 1H), 8.87 (d, *J* = 4.5 Hz, 1H), 8.57 (d, *J* = 4.8 Hz, 1H), 8.33 (s, 1H), 8.21 – 8.14 (m, 1H), 8.01 (t, *J* = 12.6 Hz, 2H), 7.89 – 7.82 (m, 1H), 7.78 (d, *J* = 7.9 Hz, 1H), 7.75 – 7.67 (m, 1H), 7.54 (d, *J* = 4.5 Hz, 1H), 7.33 (t, *J* = 6.2 Hz, 1H), 6.45 (s, 1H), 1.83 (s, 3H); <sup>13</sup>C NMR (100 MHz, DMSO-*d*<sub>6</sub>) δ 163.96, 151.33, 148.87, 148.09, 139.65, 137.50, 132.04, 130.56, 128.87, 126.19, 123.07, 121.87, 121.18, 119.69, 117.06, 96.32, 82.87, 70.06, 31.57. ESI-MS *m/z*: 341.2 [M + H]<sup>+</sup>.

**1-((4-(1H-pyrazol-4-yl)quinolin-6-yl)ethynyl)cyclohexan-1-ol (24e)**. Compound **24e** was prepared according to general procedure E on a 0.25 mmol scale. Purification by column chromatography (5% MeOH / DCM) afforded the title compound (35.7 mg, 0.11 mmol, 45% yield). White solid; mp 210-213 °C. HPLC analysis: retention time, 4.145 min; peak area, 97.84%. <sup>1</sup>H NMR (300 MHz, DMSO-*d*<sub>6</sub>) δ 13.41 (s, 1H), 8.87 (d, *J* = 6.0 Hz, 1H), 8.20 – 8.03 (m, 4H), 7.74 (dd, *J* = 8.7, 1.9 Hz, 1H), 7.55 (d, *J* = 4.5 Hz, 1H), 5.53 (s, 1H), 1.93 – 1.88 (m, 2H), 1.70 – 1.44 (m, 7H), 1.28 – 1.26 (m, 1H); <sup>13</sup>C NMR (75 MHz, DMSO-*d*<sub>6</sub>) δ 151.19, 147.97, 139.61, 132.17, 130.51, 128.63, 126.20, 121.82, 121.52, 117.10, 96.77, 83.05, 67.47, 25.37, 23.25. ESI-MS *m/z*: 318.3 [M + H]<sup>+</sup>.

**1-((4-(1H-pyrazol-4-yl)quinolin-6-yl)ethynyl)cyclopentan-1-ol (24f)**. Compound **24f** was prepared according to general procedure E on a 0.28 mmol scale. Purification by column chromatography (5% MeOH / DCM) afforded the title compound (55.3 mg, 0.18 mmol, 65% yield). White solid; mp 203-205 °C. HPLC analysis: retention time, 3.867 min; peak area, 99.16%. <sup>1</sup>H NMR (300 MHz, DMSO-*d*<sub>6</sub>) δ 13.41 (s, 1H), 8.87 (d, *J* = 3.0 Hz, 1H), 8.34 (s, 1H), 8.17 (d, *J* = 1.8 Hz, 1H), 8.03 (d, *J* = 8.6 Hz, 2H), 7.73 (dd, *J* = 8.7, 1.8 Hz, 1H), 7.55 (d, *J* = 3.0 Hz, 1H), 5.40 (s, 1H), 1.96 – 1.89 (m, 4H), 1.80 – 1.64 (m, 4H); <sup>13</sup>C NMR (100 MHz, DMSO-*d*<sub>6</sub>) δ 151.23, 147.99, 139.59, 132.06, 130.53, 129.45, 128.66, 126.21, 121.84, 121.53, 117.08, 96.87, 81.82, 73.29, 42.42, 23.56. ESI-MS *m/z*: 304.5 [M + H]<sup>+</sup>.

**4-(4-(1H-pyrazol-4-yl)quinolin-6-yl)-2-(thiazol-2-yl)but-3-en-2-ol (24g)**. To a suspension of **23** (109.2 mg, 0.34 mmol), Pd(OAc)<sub>2</sub> (3.8 mg, 5% mmol), PPh<sub>3</sub> (17.8 mg, 20% mmol) and the corresponding 2-(thiazol-2-yl)but-3-en-2-ol (105.5 mg, 0.68 mmol) in toluene (3.5 mL), Et<sub>3</sub>N (0.68 mL) was added. The resulting mixture was refluxed and stirred overnight. After the reaction was completed, the mixture was evaporated in vacuo. The

residue was chromatographed, eluting with a gradient of (DCM / MeOH = 20: 1) to afford title compound **24** (48.8 mg, 0.14 mmol, 41%, yield). Yellow solid; mp 299-201 °C. HPLC analysis: retention time, 4.365 min; peak area, 97.42%. <sup>1</sup>H NMR (300 MHz, DMSO-*d*<sub>6</sub>) δ 13.37 (s, 1H), 8.96 – 8.28 (m, 2H), 8.25 – 7.86 (m, 4H), 7.85 – 7.42 (m, 3H), 7.08 – 6.64 (m, 2H), 6.49 (d, *J* = 4.8 Hz, 1H), 1.76 (d, *J* = 4.7 Hz, 3H). ESI-MS *m/z*: 349.4 [M + H]<sup>+</sup>. <sup>13</sup>C NMR (100 MHz, DMSO-*d*<sub>6</sub>) δ 179.23, 150.31, 148.53, 142.95, 139.65, 137.34, 135.15, 130.49, 127.20, 127.06, 126.36, 124.29, 121.35, 120.20, 117.38, 74.82, 29.87. ESI-MS *m/z*: 349.4 [M + H]<sup>+</sup>.

### General Procedure F for the Synthesis of Compounds **27a**—**27b**.

To a stirred ice-cooled solution of **25** (124.1 mg, 0.4 mmol) in dry DMF (1.2 mL), the corresponding five-membered ring functionalized carbonyl chloride (0.44 mmol, 1.1 equiv) in dry DMF was added dropwise under N<sub>2</sub> atmosphere. Subsequently, Et<sub>3</sub>N (1.0 mmol, 2.0 equiv) in DMF (1.5 mL) was added dropwise. The mixture was allowed to reach room temperature and stirred for 2.0 h. The mixture was extracted with EA (30 mL × 3). The combined organic layers were washed with brine, dried over Na<sub>2</sub>SO<sub>4</sub>, and concentrated under vacuum. Following the corresponding part of the general procedure B, the “-Boc” protecting group of crude product **26** was removed. The obtained residue was chromatographed, eluting with a gradient of (DCM / MeOH = 20: 1) to afford title compound **27a**–**27b** (yield, 43–53%) as a white or yellow solid.

**N-(4-(1H-pyrazol-4-yl)quinolin-6-yl)thiazole-2-carboxamide (27a)**. Compound **27a** was prepared according to general procedure F on a 0.4 mmol scale. Purification by column chromatography (5% MeOH / DCM) afforded the title compound (55.1 mg, 0.17 mmol, 43% yield). Yellow solid; mp 215-217 °C. HPLC analysis: retention time, 3.643 min; peak area, 96.14%. <sup>1</sup>H NMR (300 MHz, DMSO-*d*<sub>6</sub>) δ 13.40 (s, 1H), 11.28 (s, 1H), 8.94 (d, *J* = 2.3 Hz, 1H), 8.79 (d, *J* = 4.6 Hz, 1H), 8.31 (dd, *J* = 9.1, 2.3 Hz, 2H), 8.25 – 8.12 (m, 3H), 8.05 (d, *J* = 9.1 Hz, 1H), 7.57 (d, *J* = 4.6 Hz, 1H). <sup>13</sup>C NMR (100 MHz, DMSO-*d*<sub>6</sub>) δ 164.20, 158.63, 149.46, 145.90, 144.55, 139.40, 136.89, 130.25, 127.32, 126.15, 124.38, 120.86, 117.59, 115.29. ESI-MS *m/z*: 322.4 [M + H]<sup>+</sup>.

**N-(4-(1H-pyrazol-4-yl)quinolin-6-yl)cyclopentanecarboxamide (27b)**. Compound **27a** was prepared according to general procedure F on a 0.4 mmol scale. Purification by column chromatography (6% MeOH / DCM) afforded the title compound (65.5 mg, 0.21 mmol, 53% yield). White solid; mp 283-285 °C. HPLC analysis:

retention time, 3.741 min; peak area, 98.93%.  $^1\text{H}$  NMR (300 MHz,  $\text{DMSO-}d_6$ )  $\delta$  13.35 (s, 1H), 10.25 (s, 1H), 8.75 (dd,  $J = 15.8, 3.4$  Hz, 2H), 8.29 (s, 1H), 8.09 – 7.87 (m, 3H), 7.50 (d,  $J = 4.6$  Hz, 1H), 2.84 (t,  $J = 7.7$  Hz, 1H), 1.95 – 1.51 (m, 8H).  $^{13}\text{C}$  NMR (75 MHz,  $\text{DMSO-}d_6$ )  $\delta$  175.32, 148.93, 145.65, 138.78, 138.16, 130.46, 126.49, 123.29, 120.91, 117.77, 112.86, 45.91, 30.57, 26.19. ESI-MS  $m/z$ : 307.2  $[\text{M} + \text{H}]^+$ .

**2-methyl-4-(4-(1-methyl-1H-pyrazol-4-yl)quinolin-6-yl)but-3-yn-2-ol (28)**. Compound **28** was prepared according to general procedure E on a 0.4 mmol scale. Purification by column chromatography (6% MeOH / DCM) afforded the title compound (74.6 mg, 0.26 mmol, 64% yield). White solid; mp 118-120 °C. HPLC analysis: retention time, 3.682 min; peak area, 99.15%.  $^1\text{H}$  NMR (300 MHz,  $\text{DMSO-}d_6$ )  $\delta$  8.87 (s, 1H), 8.30 (s, 1H), 8.16 (s, 1H), 8.03 (d,  $J = 9.0$  Hz, 1H), 7.90 (s, 1H), 7.72 (d,  $J = 6.0$  Hz, 1H), 7.52 (s, 1H), 5.54 (s, 1H), 3.99 (s, 3H), 1.50 (s, 6H).  $^{13}\text{C}$  NMR (100 MHz,  $\text{DMSO-}d_6$ )  $\delta$  151.24, 148.00, 139.24, 139.21, 132.21, 131.56, 130.55, 128.48, 126.06, 121.68, 121.48, 117.66, 97.86, 80.83, 64.19, 32.01. ESI-MS  $m/z$ : 292.1  $[\text{M} + \text{H}]^+$ . ASSOCIATED CONTENT

The following files are available free of charge.

The reagents and antibodies used for biological evaluation in vitro or vivo.  $^1\text{H}$  NMR and  $^{13}\text{C}$  NMR spectra for target compounds. The HPLC spectra for target compounds. (.pdf)

Authors will release the atomic coordinates and experimental data upon article publication.

## AUTHOR INFORMATION

### Corresponding Authors

\*(Tao Lu) Tel: +86-25-86185180; Fax: +86-25-86185179; E-mail: lutao@cpu.edu.cn

\*(Yadong Chen) Tel: +86-25-86185153; Fax: +86-25-861851170; E-mail: ydchen@cpu.edu.cn

### Author Contributions

<sup>†</sup>Jianing Song and Yuqin Zhu contributed equally to this work. The authors declare no competing financial interest. The manuscript was written through contributions of all authors.

## ACKNOWLEDGMENT

This study was supported by grants from the National Natural Science Foundation of China (Grant No. 81973182, 81673301) ; "Double First-Class" University project from China Pharmaceutical University (Program No. CPU2018GF02). We thank Prof. Lei Qiang, China Pharmaceutical University, for technical assistance of pharmacology.

## ABBREVIATIONS

NIK, Nuclear factor kappa-B inducing kinase; NF- $\kappa$ B, Nuclear factor kappa-light-chain-enhancer of activated B cells; TNFSFR, Tumor necrosis factor superfamily receptor; CD40, Cluster of differentiation 40; CD40L, Cluster of differentiation 40 ligand; TRAF3, Tumor necrosis factor receptor-associated factor 3; BAFF, B-cell activating factor; BAFF-R, B-cell activating factor receptor; Fn14 (TWEAK-R or TNFRSF12A), Tumor necrosis factor receptor superfamily member 12A; TRAF2-clAPs, Tumor necrosis factor receptor (TNFR)-associated factor 2-Cellular Inhibitor of apoptosis proteins; IKK $\alpha$ , I $\kappa$ B kinase  $\alpha$ ; IMQ, Imiquimod.

## REFERENCES

1. Verma IM, Stevenson JK, Schwarz EM, et al. Rel/NF-kappa B/I kappa B family: intimate tales of association and dissociation. *Genes Dev.* 1995;9:2723-2735.
2. Ghosh S, May MJ, Kopp EB. NF-kappa B and Rel proteins: evolutionarily conserved mediators of immune responses. *Annu Rev Immunol.* 1998;16:225-260.
3. Liu T, Zhang L, Joo D, et al. NF- $\kappa$ B signaling in inflammation. *Signal Transduct Target Ther.* 2017;2:17023-.
4. Li Q, Verma IM. NF-kappaB regulation in the immune system. *Nat Rev Immunol.* 2002;2:725-734.
5. Beinke S, Ley SC. Functions of NF-kappaB1 and NF-kappaB2 in immune cell biology. *Biochem J.* 2004;382:393-409.
6. Vallabhapurapu S, Karin M. Regulation and function of NF-kappaB transcription factors in the immune system. *Annu Rev Immunol.* 2009;27:693-733.
7. Hayden MS, West AP, Ghosh S. NF-kappaB and the immune response. *Oncogene.* 2006;25:6758-6780.
8. Neurath MF, Pettersson S, Meyer zum Büschenfelde KH, et al. Local administration of antisense phosphorothioate oligonucleotides to the p65 subunit of NF-kappa B abrogates established experimental colitis in mice. *Nat Med.* 1996;2:998-1004.
9. Sil AK, Maeda S, Sano Y, et al. I $\kappa$ B kinase- $\alpha$  acts in the epidermis to control skeletal and craniofacial morphogenesis. *Nature.* 2004;428:660-664.
10. Lavon I, Goldberg I, Amit S, et al. High susceptibility to bacterial infection, but no liver dysfunction, in mice compromised for hepatocyte NF-kappaB activation. *Nat Med.* 2000;6:573-577.
11. Swinney DC, Xu YZ, Scarafia LE, et al. A small molecule ubiquitination inhibitor blocks NF-kappa B-dependent cytokine expression in cells and rats. *J Biol Chem.* 2002;277:23573-23581.
12. Willmann KL, Sacco R, Martins R, et al. Expanding the interactome of the noncanonical NF- $\kappa$ B signaling pathway. *J Proteome Res.* 2016;15:2900-2909.
13. Ramakrishnan SK, Zhang H, Ma X, et al. Intestinal non-canonical NF $\kappa$ B signaling shapes the local and systemic immune response. *Nat Commun.* 2019;10:660.

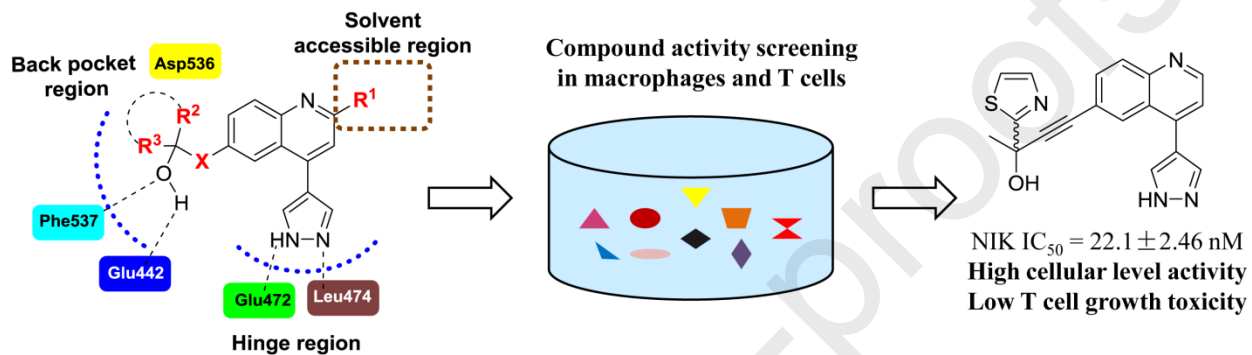
14. Sun SC. The non-canonical NF- $\kappa$ B pathway in immunity and inflammation. *Nat Rev Immunol*. 2017;17:545-558.
15. Ishimaru N, Kishimoto H, Hayashi Y, et al. Regulation of naive T cell function by the NF-kappaB2 pathway. *Nat Immunol*. 2006;7:763-772.
16. Noort AR, Tak PP, Tas SW. Non-canonical NF- $\kappa$ B signaling in rheumatoid arthritis: Dr Jekyll and Mr Hyde? *Arthritis Res Ther*. 2015;17:15.
17. Noort AR, van Zoest KP, Weijers EM, et al. NF- $\kappa$ B-inducing kinase is a key regulator of inflammation-induced and tumour-associated angiogenesis. *J Pathol*. 2014;234:375-385.
18. Baum R, Gravalles EM. Bone as a target organ in rheumatic disease: impact on osteoclasts and osteoblasts. *Clin Rev Allergy Immunol*. 2016;51:1-15.
19. Wei F, Chang Y, Wei W. The role of BAFF in the progression of rheumatoid arthritis. *Cytokine*. 2015;76:537-544.
20. Petri M, Stohl W, Chatham W, et al. Association of plasma B lymphocyte stimulator levels and disease activity in systemic lupus erythematosus. *Arthritis Rheum*. 2008;58:2453-2459.
21. Li Y, Wang H, Zhou X, et al. Cell intrinsic role of NF- $\kappa$ B-inducing kinase in regulating T cell-mediated immune and autoimmune responses. *Scientific Reports*. 2016;6:22115.
22. Simmons SB, Pierson ER, Lee SY, et al. Modeling the heterogeneity of multiple sclerosis in animals. *Trends Immunol*. 2013;34:410-422.
23. Banoth B, Chatterjee B, Vijayaragavan B, et al. Stimulus-selective crosstalk via the NF- $\kappa$ B signaling system reinforces innate immune response to alleviate gut infection. *eLife*. 2015;4:e05648.
24. Etemadi N, Chopin M, Anderton H, et al. TRAF2 regulates TNF and NF- $\kappa$ B signalling to suppress apoptosis and skin inflammation independently of sphingosine kinase 1. *eLife*. 2015;4:e10592.
25. Mair F, Joller S, Hoeppli R, et al. The NF- $\kappa$ B-inducing kinase is essential for the developmental programming of skin-resident and IL-17-producing  $\gamma\delta$  T cells. *eLife*. 2015;4:e10087.

26. Eshima K, Okabe M, Kajiura S, et al. Significant involvement of nuclear factor- $\kappa$ B-inducing kinase in proper differentiation of  $\alpha\beta$  and  $\gamma\delta$  T cells. *Immunology*. 2014;141:222-232.
27. El Malki K, Karbach SH, Huppert J, et al. An alternative pathway of imiquimod-induced psoriasis-like skin inflammation in the absence of interleukin-17 receptor a signaling. *J Invest Dermatol*. 2013;133:441-451.
28. Lin WJ, Su YW, Lu YC, et al. Crucial role for TNF receptor-associated factor 2 (TRAF2) in regulating NF- $\kappa$ B2 signaling that contributes to autoimmunity. *Proc Natl Acad Sci U S A*. 2011;108:18354-18359.
29. Zhu YQ, Ma YX, Zu WD, et al. Identification of N-phenyl-7H-pyrrolo[2,3-d]pyrimidin-4-amine derivatives as novel, potent, and selective NF- $\kappa$ B inducing kinase (NIK) inhibitors for the treatment of psoriasis. *J Med Chem*. 2020;63:6748-6773.
30. Demchenko YN, Brents LA, Li Z, et al. Novel inhibitors are cytotoxic for myeloma cells with NF- $\kappa$ B inducing kinase-dependent activation of NF- $\kappa$ B. *Oncotarget*. 2014;5:4554-4566.
31. Ren X, Li X, Jia L, et al. A small-molecule inhibitor of NF- $\kappa$ B-inducing kinase (NIK) protects liver from toxin-induced inflammation, oxidative stress, and injury. *Faseb j*. 2017;31:711-718.
32. Li Z, Li X, Su MB, et al. Discovery of a potent and selective NF- $\kappa$ B-inducing kinase (NIK) inhibitor that has anti-inflammatory effects in vitro and in vivo. *J Med Chem*. 2020;63:4388-4407.
33. Vancurova I, Vancura A. Regulation and function of nuclear I $\kappa$ B $\alpha$  in inflammation and cancer. *Am J Clin Exp Immunol*. 2012;1:56-66.
34. Kojima H, Aizawa Y, Yanai Y, et al. An essential role for NF-kappa B in IL-18-induced IFN-gamma expression in KG-1 cells. *J Immunol*. 1999;162:5063-5069.
35. Huang Z-b, Zheng Y-x, Li N, et al. Protective effects of specific cannabinoid receptor 2 agonist GW405833 on concanavalin A-induced acute liver injury in mice. *Acta Pharmacol Sin*. 2019;40:1404-1411.
36. Brightbill HD, Suto E, Blaquiere N, et al. NF- $\kappa$ B inducing kinase is a therapeutic target for systemic lupus erythematosus. *Nat. Commun*. 2018;9:179.
37. Van Oeveren A, Motamedi M, Martinborough E, et al. Novel selective androgen receptor modulators: SAR studies on 6-bisalkylamino-2-quinolinones. *Bioorganic Med. Chem. Lett*. 2007;17:1527-1531.

38. Mao L, Bertermann R, Emmert K, et al. Synthesis of vinyl-, allyl-, and 2-boryl allylboronates via a highly selective copper-catalyzed borylation of propargylic alcohols. *Org Lett.* 2017;19:6586-6589.

39. Boga C, Stengel R, Abdayem R, et al. Regioselectivity in the addition of vinylmagnesium bromide to heteroaryl ketones: C- versus O-alkylation. *J Org Chem.* 2004;69:8903-8909.

### Graphical Abstract



## Graphical Abstract

